

BIROn - Birkbeck Institutional Research Online

Ketcham, R.A. and Carter, Andrew and Hurford, A.J. (2015) Inter-laboratory comparison of fission track confined length and etch figure measurements in apatite. *American Mineralogist* 100 (7), pp. 1452-1468. ISSN 0003-004X.

Downloaded from: <https://eprints.bbk.ac.uk/id/eprint/13146/>

Usage Guidelines:

Please refer to usage guidelines at <https://eprints.bbk.ac.uk/policies.html>
contact lib-eprints@bbk.ac.uk.

or alternatively

Inter-Laboratory Comparison of Fission Track Confined Length and Etch Figure Measurements in Apatite

Richard A. Ketcham¹, Andrew Carter², Anthony J. Hurford³

¹Jackson School of Geosciences, The University of Texas at Austin, Austin, TX, USA

²Department of Earth and Planetary Sciences, Birkbeck College, Malet Street, London, WC1E 7HX, UK.

³Department of Earth Sciences, University College, Gower Street, London, WC1E 6BT, UK,

Key words: GEOCHRONOLOGY: fission-track dating, track length measurement, apatite, inter-laboratory calibration, thermal history analysis

Abstract

Apatite fission-track length and etch figure data are powerful tools for obtaining thermal history information, but both require human analysts making manual measurements, and reproducibility is not assured. We report the results of an inter-laboratory study designed to clarify areas of congruence and divergence for these measurements and provide a basis for evaluating best practices to enhance intercompatibility of data sets. Four samples of megacrystic apatite from Durango, Mexico with induced tracks, one unannealed and three thermally annealed by varying amounts, were distributed internationally. In all, 55 analysts in 30 laboratory groups participated in the experiment. Relative mean track lengths among the samples were consistent across all analysts, but measurements for each sample showed scatter among labs and analysts considerably in excess of statistical expectation. Normalizing measurements of annealed samples using the unannealed sample improved consistency, as did normalizing for track angle using c-axis projection. Etch figure data also showed variability

beyond statistical expectation, and consistency was improved by normalizing. Based on these data we recommend rigorous analyst training for length and etch figure measurement that includes measurement of standards, and that each analyst's data on unknowns be normalized by that analyst's own measurements on standards when using thermal history inverse modeling as part of the interpretation process.

Introduction

The key to resolving detailed thermal histories using the apatite fission-track (AFT) system comes from combining ages with track length data. Fission tracks form over time, and earlier-formed ones will experience more of a sample's thermal history than later-formed ones. This leads to characteristic patterns in horizontal confined track length distributions that can provide unique information on thermal history (Gleadow *et al.*, 1986). Even greater resolution is available when length data are paired with computational tools (e.g., Gallagher, 1995; Gallagher, 2012; Green *et al.*, 1989; Ketcham, 2005) to identify the range of thermal histories that are consistent with both the length and age data and other geological constraints, using kinetic models of fission-track annealing (Crowley *et al.*, 1991; Ketcham *et al.*, 2007b; Ketcham *et al.*, 1999; Laslett and Galbraith, 1996; Laslett *et al.*, 1987).

The ability to use track length data correctly and confidently hinges on the fidelity of the length measurements, and in particular their consistency with respect to the measurements underlying models of fission-track annealing (e.g., Barbarand *et al.*, 2003a; Carlson *et al.*, 1999; Green *et al.*, 1986). Although the analytical procedures used in these studies can be reproduced, and we understand many of the geometric sources of bias associated with track observation (Galbraith, 2005 Chapter 8; Galbraith *et al.*, 1990; Ketcham, 2003), full compatibility is not assured. In particular, because confined tracks are found and measured by a human analyst using

a microscope, rather than some mechanical or automated procedure, reproducibility of length data is an important concern.

The reproducibility of confined length data has been considered at both the inter-lab and intra-lab level. Intra-lab studies are valuable because they enable better control of conditions (such as repeating measurements of the same material using the same instrumentation), and thus allow focus on variables of interest. For example Green et al. (1986) include and compare measurements by two analysts of the same mounts. Barbarand et al. (2003b) gathered a series of induced-track data aimed at examining various aspects of reproducibility in detail, including among analysts and for single analysts over time, as well as the effects of Cf irradiation and the number of measurements necessary to converge to the correct mean length. Ketcham et al. (2009) obtained data for several analysts on two samples with induced and spontaneous tracks, and assessed the effects of measurement variability on thermal history reconstruction and the potential mediating ability of normalizing for length and angle.

Inter-laboratory experiments, however, provide the information necessary to assess the fidelity of measurements across the community and thus the overall reliability of the technique as it is applied. There has only been one previous large-scale inter-laboratory experiment for length measurements (Miller *et al.*, 1993), and its outcome was mixed, indicating general agreement but scatter substantially in excess of statistical expectation. Definitive interpretation was complicated, however, because the material was non-ideal, consisting of aliquots of natural samples with spontaneous fission tracks, which could conceivably have been non-homogeneous. Also, no information was reported about laboratory techniques, such as etching method.

With the help and cooperation of the international AFT community, we have performed a new inter-laboratory experiment designed to gather information intended to clarify areas of

congruence and divergence, provide a basis for evaluating best practices to enhance intercompatibility of data sets, and suggest areas that merit further study.

Methodological Overview

Length revelation

Fission tracks are too narrow (8-9 nm diameter in apatite; Li *et al.*, 2010) to be observed under an optical microscope, and instead are revealed by their ability to etch more easily than bulk crystal. Fission-track mounts are prepared by mounting grains in epoxy, polishing to reveal interior surfaces, and then etching in nitric acid (HNO₃) at some prescribed conditions of strength, temperature and duration. Apatite etches anisotropically (Green and Durrani, 1977), with faster etching in the direction of the crystallographic *c* axis, and in general stronger etchants (higher concentration and/or temperature) are expected to increase this anisotropy compared to weaker ones.

Fission tracks intersecting the polished surface only contain partial length information, as one of their ends is missing. Confined tracks are revealed when etchant travels down a pathway from the exposed surface and intersects a track in which both ends are within the solid crystal. When the etchant pathway is another fission track, the confined track is referred to as a TINT (track-in-track; Lal *et al.*, 1969), while if the pathway is a fracture or cleavage it is termed a TINCLE (track-in-cleavage, Bhandari *et al.*, 1971).

Length measurement

Confined track lengths are measured under a microscope at high magnification, generally 1000x-1600x, using either a drawing tube and digitizing tablet or a camera and specialized software to measure the distance between track ends. As surface etch rates vary according to

crystallographic orientation it is normal practice to control for etching efficiency and measure tracks only on grains in which the crystallographic *c* axis is in the polished plane, as these have the lowest bulk etch rate. *C*-parallel sections can be determined by their aligned etch figures (Donelick *et al.*, 2005), and track orientation with respect to the *c* axis can be determined as the angle between the track and the etch figure elongation direction. Confined tracks must be close to horizontal, although limited inclination has little effect; the projection of a track dipping 10° with respect to the polished surface is within a factor of $\cos(10^\circ)$, or 0.985, of the true length. It is also possible to measure steeper tracks if the measurement system records the 3D location of the endpoints and accounts for the apatite refractive index, allowing a correction to be made, although one test has found non-horizontal tracks to slightly increase the standard deviation of the length distribution (Jonckheere and Ratschbacher, 2010).

For a fission track to be considered measurable, it must be completely etched, with clearly defined ends. The revelation of a track will depend on its angle relative to the *c* axis (hereafter denoted as ϕ) and the etching protocol; examples are shown in Figure 1. When a strong etchant (5.0 or 5.5 M) is used, tracks are most easily observed, and more likely to be fully etched, when they are in the ϕ range of approximately 30-85° (Fig. 1A,B) (Barbarand *et al.*, 2003b; Donelick *et al.*, 1999). Tracks at lower angles (Fig. 1C, D track 1; 1E track 1) are thin for their entire extent. Tracks close to perpendicular to the *c* axis ($\phi > 85^\circ$) can look wide but slightly distorted (Fig. 1E, track 2) or initially wide near the intersection with the etchant pathway and pinched toward the ends (Fig. 1F). The distorted shape of track 2 in Fig. 1E may result in a slight error in angle determination when the line connecting the endpoints is not parallel to the length. In the case of thin or pinched tracks, the ends can be indistinct, making it difficult to tell whether they are fully etched or not; under-etched tracks should not be measured because they

may not record the full length, and instead could give a spurious signal of track shortening. These etching effects, combined with the anisotropy of TINT etchant pathways, impart a substantial bias upon which angular populations are measured (Galbraith et al., 1990; Ketcham, 2003).

The anisotropy in etching diminishes for a weaker etchant (e.g. $<2\text{N HNO}_3$), reducing somewhat the dissimilarity of confined tracks at different ϕ angles. However, weaker etchants require longer etching times ($>40\text{s}$ vs. 20s), and etching duration brings up additional considerations (Jonckheere et al., 2007; O'Sullivan et al., 2004). There is inevitably some time delay before confined tracks start to etch, which varies depending on the strength of the etchant, extent of subsurface penetration along a pathway (TINT or TINCLE) and solubility (composition) of the apatite. As a result, even tracks at favorable angles can be under-etched, and the variability in etching time contributes to variation in measured track lengths. For similar reasons, short tracks are somewhat more likely to be fully etched than otherwise equivalent longer tracks, partially counter-acting the biasing effect of longer lengths being more likely to be intersected and etched than shorter ones (Laslett *et al.*, 1982).

Other situations that can lead to erroneous measurements are shallow tracks that intersect the polished surface (Fig. 1C,D track 2), tracks with fluid-filled and thus obscured ends (Fig. 1G,H) and opposite-dipping semi-track pairs that appear superficially to be single tracks. Of these cases, the first two will lead to erroneously short measurements, and the third can be either short or long.

The analyst measuring fission tracks must thus constantly keep in mind, and adhere to, strict criteria for determining which confined tracks should be measured and which should be bypassed. There is likely to be some variability in these criteria between analysts and lab groups,

which will contribute to variation. Finally, measurement by microscopy or via stored digital images requires some form of calibration. Methods employed include calibrated microscope scale bars (typically at 1-2 μm resolution) or SEM diffraction gratings (typically < 0.4-0.6 μm resolution). Calibration should be made only for the area in which the features to be measured are placed. Typically this is in the center of the field of view in order to avoid the defocused peripheral regions. Systems that use digitizing tablets are also vulnerable to models that have an uneven spacing of grid wires. Another potential issue when a drawing tube is employed is the size of the LED spot used to demark track ends; most analysts center the spot over the ends, but some use an edge of the spot to attempt to make the measurement more precise. All of these aspects can contribute to systematic differences between laboratories.

C-axis projection

In addition to anisotropy of etching, apatite fission tracks also show annealing anisotropy, with tracks parallel to the **c** axis annealing more slowly than tracks oriented along the **a** axis (Donelick, 1991; Donelick et al., 1999; Green and Durrani, 1977). At low to medium amounts of annealing, annealing rates vary smoothly between these two orientations, and length distributions are well-represented as ellipses on a polar plot (Donelick, 1991), although in detail the distribution may be slightly non-elliptical (Jonckheere et al., 2007). At high levels of annealing, tracks at high ϕ angles begin to shorten much more quickly and disappear while low- ϕ tracks persist, a process termed accelerated length reduction (Donelick et al., 1999).

As annealing progresses, annealing anisotropy leads to greatly increased dispersion in lengths of tracks that have experienced identical amounts of heating, as shown in experiments in which induced tracks are annealed (e.g., Green et al., 1986). To compensate for this, Donelick et al. (1999) introduced **c**-axis projection, which was subsequently refined by Ketcham (2003) and

Ketcham et al. (2007a). **C**-axis projection is a transform that converts each (l, ϕ) measurement into an estimate of what the length of a track oriented along the **c** axis that had experienced the same annealing conditions would be, l_c , and the uncertainty in that estimate, σ_{l_c} . It can be more generally viewed as a means of removing the dispersion caused by annealing anisotropy, resulting in a more precise index of thermal input for a given track than length alone.

Creating a **c**-axis projection model consists of fitting ellipse radii, $l_{c,fit}$ and $l_{a,fit}$ corresponding to the **c**-axis and **a**-axis directions, to sets of tracks measured in a series of experimental annealing runs. These data are then used to fit a four-parameter projection transform (Ketcham et al., 2007a). This process generally requires dozens of experiments to document all stages of annealing and overcome dispersion in the ellipse fits, and thus has only been done on the two largest experimental data sets, by Carlson et al. (1999) and Barbarand et al. (2003a). These studies used slightly different etchant strengths, respectively 5.5 M and 5.0M HNO_3 , and the difference between their respective **c**-axis projection models was attributed to etchant (Ketcham et al., 2007a). The present study tests whether this assertion is correct, or some other factor may be responsible for variation in observed anisotropy effects.

Etch figures

Etch figures, the intersections of etched tracks with the polished surface (Fig. 1D), are useful for determining crystallographic orientation, as a proxy for inferring the effective annealing kinetics (Burtner *et al.*, 1994; Ketcham *et al.*, 1999) and estimating initial (unannealed) track length (Carlson *et al.*, 1999). The principal measured parameter is the diameter of the track parallel to the apatite **c** axis when it is in the polished plane (D_{par}); the **c**-axis perpendicular diameter, D_{per} , is also of potential use, but is more difficult to measure reliably. The Ketcham et al. (2009) experiment found reproducibility among multiple analysts

measuring D_{par} on the same grain mounts to be poor. Sobel and Seward (2010) studied the problem under better conditions and in considerably more detail, and suggest protocols for executing and normalizing D_{par} measurements.

Methods

Preparations for the experiment began in 2004. Mark Cloos (University of Texas at Austin) provided a selection of lime-colored apatite crystals from Durango, Mexico, and three were selected as containing minimal defects. Each was heated at 500°C for 24 hours to totally anneal spontaneous tracks. Aliquots of each crystal were polished, etched and inspected to confirm total spontaneous track removal. Each crystal was sliced into ~1 mm plates parallel to the *c*-axis using a fine diamond saw. The sliced crystals were wrapped in aluminum foil and irradiated at the Lucas Heights reactor (Australia) in April 2004 using nominal thermal neutron fluences of $2 \times 10^{16} \text{ ncm}^{-2}$. Each crystal was irradiated in a separate reactor run (TE68, 70 and 77) to keep the total mass of active material within acceptable limits. Each irradiation was monitored by inclusion of a CN-5 dosimeter glass with a mica detector. Substantial radioactivity was allowed to decay until early 2008.

In 2008, induced tracks in the samples were partially annealed and aliquots distributed to participating laboratories. Apatite from irradiation TE70 was designated DUR-1, apatite from irradiation TE77 was divided into two aliquots designated DUR-2 and DUR-3, and apatite from irradiation TE68 was designated DUR-4. Appropriate annealing conditions were estimated based on Barbarand et al. (2003a), and the furnaces, annealing rig, thermocouples and all procedures were identical to those used by Barbarand et al. (2003a).

For sample DUR-1 annealing conditions of $288 \pm 2^\circ\text{C}$ and 10 hr (plus ~3 min equilibration time on loading) were chosen to produce a track-length distribution similar to exhumed

206 basement, with a mean length (l_m) of 11.5-12 μm . Measurements of a test aliquot gave an l_m of
207 $12.05 \pm 0.07 \mu\text{m}$ (n=100). Sample DUR-2 was left unannealed as a control sample containing
208 full-length induced tracks. For sample DUR-3 the aim was to produce a broad track-length
209 distribution as might be found in a subsurface sample, more complex to measure but with a
210 statistically-adequate number of tracks. It was annealed at $310 \pm 2^\circ\text{C}$ for 10 hr (equilibration on
211 loading took about 3.5 min), and an initial test aliquot gave an l_m of $10.20 \pm 1.10 \mu\text{m}$ (n=101).
212 DUR-4 was intended to simulate a volcanic-cooling type track-length distribution. It was
213 annealed at $240 \pm 2^\circ\text{C}$ for 10 hr (equilibration on loading took about 2 min), and an initial test
214 aliquot gave an l_m of $13.80 \pm 0.80 \mu\text{m}$ (n=102).

215 Part of the intention behind using single apatite crystals was to attempt to overcome
216 compositional variation between different grains of a large apatite concentrate. However, sample
217 compositional heterogeneity within a single crystal could still produce variation between results.
218 To help monitor such variation, the cut plates of each apatite were broken and the relative
219 positions of each sub-piece recorded by simple letter-number co-ordinates (e.g. A1, C5 etc).
220 Where possible each lab was sent the aliquots for each apatite (DUR 1,2,3&4) taken from the
221 same relative position (A1, C5 etc.); however, this system broke down in later distributions when
222 inadequate orientated material remained.

223 Fission-track laboratories known to the authors were contacted and aliquots provided to
224 those who agreed to participate. All preparation of grain mounts and measurement was done at
225 each participating laboratory using its standard operating procedures and instrumentation. A
226 survey (Supplementary Data) was also prepared to accompany all aliquots, so that laboratories
227 could report pertinent information such as etching procedures, measurement systems, and analyst
228 experience as of the time of the measurement. Survey answers are summarized in Table 1.

Results were returned by email. Each data set by a single analyst for a single sample was given a code (1-4)-L(1-47)-A(1-6)[-Q(1-3)], where the first number indicates the DUR sample number, the second is the laboratory group, the third is the analyst at that laboratory, and the “Q” designation is used as needed when the analyst measured the same sample multiple times (example: 1-L13-A2-Q1 refers to sample DUR-1 analyzed by lab 13, analyst 2, first measurement).

Summary statistics were calculated for all data submitted. The angular distribution of tracks in each measurement for which angle data were reported was analyzed by fitting polar-plot ellipses to provide the intercepts with crystallographic **c** and **a** axes ($l_{c,fit}$, $l_{a,fit}$), following the method of Donelick (1991) and Donelick et al. (1999). In results for DUR-3 that showed evidence of accelerated length reduction, the shortened tracks, generally those $<7\text{-}7.5\text{ }\mu\text{m}$ at high ϕ angles, were removed for ellipse fitting; numbers ranged from 0 to 16 deleted measurements, the average was 2 per experiment (or 1.7% of tracks measured), and the median was 1.

We also calculated $l_{c,mod}$, the mean of individually **c**-axis-projected lengths, using the two models given in Ketcham et al. (2007a), which characterize the Carlson et al. (1999) and Barbarand et al. (2003a) data sets; for brevity, these are respectively referred to as the C99 and B03 projection models in the discussion below. Which of these two models more closely represents the tendencies of a given analyst may be evaluated by the extent to which $l_{c,fit}$ and $l_{c,mod}$ match, or in how they co-evolve with increasing annealing.

Results

In all, 30 laboratory groups participated in the experiment, with 55 analysts in total, 53 of which provided analyses of all four samples.

To evaluate variability among aliquots, two analysts in lab 32 measured three separate aliquots. Lab 32 also included a virtually untrained analyst (number 4), who received only enough instruction to recognize a track and measure it, as an intentional end-member case of minimal experience.

Some laboratory groups independently decided to conduct additional measurements to capture additional information. Lab 13 re-polished and re-etched each mount three times with different etching protocols to inspect etching effects. Three analysts in lab 14 measured both TINT and TINCLE tracks and provided summaries for each; all results are reported, but for comparing among lab groups we utilize the combined results. Lab 41 performed measurements with and without ^{252}Cf irradiation (Donelick and Miller, 1990) to enhance detection of confined tracks.

Survey

Responses to the survey are provided in Table 1. We requested for one survey to be submitted per analyst, although some lab groups submitted combined surveys, and others omitted some questions or neglected to submit them. Experience of users represents a full continuum from 38 years of experience to novice. Among those who reported at least 1 year of experience, the mean was 12.5 years.

Results indicate a number of areas of congruence in the community. Only one lab uses oil-immersion microscopy, and almost all used the straightforward method of demarking track ends directly with an LED or pointer when measuring, as opposed to previously mentioned strategies aimed at compensating for non-negligible LED size. Most analysts measured only TINT tracks to avoid uncertainties associated with fracture movement that could increase the apparent length of tracks and to avoid additional orientation bias (since cleavage in apatite is

oriented at {0001} and {1010}), as well as the possibility that geologic fluids could have infiltrated and pre-etched or otherwise fixed tracks at some earlier stage in their history (Jonckheere and Wagner, 2000).

Results showed an unexpected diversity of etching protocols, however. In all 14 different protocols were reported, although two of these were experiments intended to test etching effects, and one was an adapted procedure intentionally analogous to that used for zircon (e.g., Yamada et al., 1995). Seven employed 5.0 or 5.5 M HNO₃ at slightly different temperatures; seven used other etchant strengths. The number of track lengths measured on each sample varied among labs and samples, from 50 to over 200.

Unannealed sample, mean length

There was considerable variation among results for the unannealed sample, DUR-2. Data are given in Table 2, and mean track lengths and errors are plotted against several variables in Figure 2. Excluding four outliers below 15 μm , there was a spread in results of almost 1.6 μm (15.25-16.84 μm). Overall, only 23 of the 65 measurements reported (35%) are within 2 standard errors of the overall mean ($15.89 \pm 0.12 \mu\text{m}$).

Experience and frequency of making measurements do not seem to be factors contributing to consistency of results; the most-frequent analysts (lab 13) differed from the second-most frequent (lab 14) by well over 1 μm (Fig. 2B). There is a vague trend of increasing mean length versus operators' frequency of analyses and years of experience (Fig. 2B, C), but overall the data are scattered in this regard.

Interestingly, there is no evidence of a trend in initial length versus etching protocol, and in particular etchant strength (Fig. 2D). Overall the amount of variation observed using the two

primary etching protocols employed currently (5.0 or 5.5 M HNO₃, 20s, 21°C) spans the range observed with different etchant strengths and temperatures and durations.

Annealed samples, mean length

Figure 3 shows the mean lengths and uncertainties reported for the annealed samples, and data are provided in Tables 3-5. The degree of scatter is similar to or somewhat worse than obtained for the unannealed sample: in order of increasing degree of annealing (DUR-4, DUR-1, DUR-3), 16 of 62 (26%), 19 of 62 (31%), and 24 of 63 (38%) reported means were within two standard errors of the respective overall means.

Angular data

Of 55 analysts, 42 reported angular data and 13 did not. The ellipse fits to each experiment are shown in Supplemental Data Figures S1-S5. For each sample, a characteristic pattern of length versus angle is observed across many laboratories and analysts. In general, results repeated patterns observed in the data of Carlson et al. (1999) and Barbarand et al. (2003a): generally an elliptical distribution, with the possible exception of the most-annealed sample DUR-3.

Two selected sets of ellipse fits for the four samples are shown in Figure 4; Fig. 4A-D show the results for a very experienced analyst from lab 32, and Fig. 4E-H show the corresponding fits for the novice user from the same lab. The measurements by the experienced analyst cluster tightly around the ellipses, while the measurements by the novice are much more scattered. Most of the novice's outliers were short compared to the experienced analyst's data, although some were long. The analysts also diverge in that there is little systematic anisotropy in the measurements of the novice, whereas the experienced analyst shows the familiar pattern of

increasing anisotropy at increasing levels of annealing (e.g., Donelick, 1991; Donelick *et al.*, 1999).

The most-annealed sample, DUR-3, experienced conditions that put it into the first stages of the “accelerated length reduction” regime (Donelick *et al.*, 1999; Ketcham *et al.*, 1999), in which tracks at high angles to the **c**-axis begin to anneal more quickly, departing from the elliptical trend. Whether these shortened tracks were measured or not was an area of particular divergence. Figure 5 shows six additional examples (to go with Fig. 4C and G), in which all analysts had at least 19 years of experiences. These analysts range from measuring zero (top row) to a few (middle row) to several (bottom row) tracks that do not fall on the elliptical trend. In some cases (e.g., labs 41, 47), different analysts observing the same mount measured very different proportions of non-elliptical tracks.

The data also show divergence in the relative frequencies of measurement of elliptical-trend high- and low- ϕ tracks. For example, some analysts measured very few high-angle ($\phi > 85^\circ$) tracks (Lab 5-A1; see Fig. S1 for examples in this paragraph), and others measured very few in the unannealed samples but more in the annealed samples (Lab 5-A2, 34, 41). Some measured very few to zero low-angle tracks ($\phi < 30\text{--}40^\circ$) in all experiments (Lab 20, 22, 30, 32-A1, 34, 41), while others measured an increasing proportion of low-angle tracks as annealing progressed (Lab 7, 13, 14, 26, 32-A2), and others measured them with roughly equivalent frequency in all samples (Lab 5, 28).

C-axis projected data

Both **c**-axis projection models provided $l_{c,mod}$ values that matched the fitted ellipses fairly well. The B03 model fits best, with a mean residual ($l_{c,fit} - l_{c,mod}$) of $-0.02\ \mu\text{m}$ and standard

deviation of 0.56 μm , whereas C99 model has a mean residual of -0.30 μm and standard deviation of 0.58 μm . The cause of this difference is made evident (Fig. 6A) by comparing the $l_{c,fit}$ vs. $l_{a,fit}$ points against the lines that define their relationship (Donelick *et al.*, 1999, Equation 1) in the two projection models. The B03 line passes through the center of the data, and the C99 line intersects a cluster of points implying a steeper slope, or more quickly increasing anisotropy with increasing annealing.

To further examine the data, lines were fitted to the four $l_{c,fit}$ vs. $l_{a,fit}$ data points for each sample by each analyst. The resulting slope and intercept parameters are shown in Figure 6B. The B03 line parameters lie in the midst of the resulting point cluster, while the C99 parameters are close to the high-slope extreme, excluding outliers.

When deriving the two *c*-axis projection models, Ketcham *et al.* (2007a) postulated that their difference in slope may be due to the difference in etchant strength, with stronger etchant leading to higher anisotropy. This idea can be tested with the data in this study by observing how slope varies with etchant across the range used in this study (Fig. 6C). Overall, we find no clear signal; the range of slopes obtained for 5.0 M HNO_3 encompasses the entire range observed for both 5.5 M HNO_3 and also weaker etchants. The strongest etchant (7 M HNO_3) appears to feature the highest slope, but those data are among the outliers. The slopes from the lab 13 experiments testing various etchant strengths by the same analysts also show no clear pattern; analyst 1 got equivalent slopes for the strongest and weakest etchants, and the highest slope for the 5.0 M HNO_3 , while analyst 2 got the lower slope for the 5.0 M and the highest for the weakest etchant. In part, these results reflect that the four-point line fits have considerable variability.

Replicate analyses

Replicate analyses by lab 32 showed no evidence of variation among aliquots. Although there was some divergence between answers beyond predicted statistical uncertainty, these were not systematic. For example, analyst 1 measured the longest mean track length on the third aliquot of sample DUR-2, whereas analyst 3 measured the shortest. On none of the four samples did they agree on the aliquot with the longest and shortest mean length. We thus conclude that variation among the apatite crystals in this study is at most a secondary effect.

TINT vs. TINCLE and ^{252}Cf irradiation

We detected no indication in the reported data, particularly those for lab 14, that TINT and TINCLE measurements systematically diverge. Similarly, measurements obtained using exclusively tracks revealed by ^{252}Cf irradiation by lab 41 analysts 2 and 5 showed no significant or systematic differences from other measurements by lab 41.

Normalization

The large degree of variation observed among laboratories and analysts is likely to be due in part to persistent factors, such as laboratory instrumentation or procedures or systematic differences in analyst training or decision-making. We thus used the results for unannealed samples (DUR-2) for each analyst to normalize results for their annealed samples.

The results of two normalizations are shown in Figure 7. Normalizing based on the mean length of DUR-2 (Fig. 7A-C) considerably increases agreement among the data. The proportions of analyses within 2 standard errors of the overall mean increase to 48%, 37%, and 49% for DUR-4, DUR-1, and DUR-3, respectively. Convergence is similar and perhaps somewhat better when the track length data are c-axis projected with the B03-based model (Fig. 7D-F), with 42%, 43%, and 52% of analyses within two standard errors of the mean. Though the comparison is

imperfect because not all analysts reported angle data, it is noteworthy that this improvement comes despite the smaller uncertainties of the c-axis projected means, which feature standard errors on average 29%, 33%, and 42% smaller for DUR-4, DUR-1, and DUR-3, respectively.

Etch figures

Figure 8 summarizes the measurements of etch figure long axis diameter (D_{par}). As with the track length data, measurements for the unannealed sample show considerable variation. Interestingly, as with the track length data, this variation does not seem to correlate with etching procedure. If one considers the two principal protocols (5.0M and 5.5M HNO₃, 20s, 21°C), it would be expected that the stronger etchant would result in larger etch figures (Sobel and Seward, 2010). However, the aggregate data do not show this (Fig. 8B).

Again, we normalized the D_{par} data for the annealed samples for each analyst using their respective measurements for sample DUR-2 (Fig. 8C). With the exception of some outliers, data for a given analyst are shown to be generally consistent to within $\pm 10\%$. The slightly lower normalized values for DUR-3 provide some indication that D_{par} may be influenced by annealing, although the effect is subtle. The lesser degrees of D_{par} shortening in the other annealed samples may be due to the less severe annealing conditions, or slight chemical variation; DUR-2 and DUR-3 are from same crystal, whereas the other experiments were from different crystals.

Discussion

Although concerns about the reproducibility of track-length data certainly arise from these experiments, the predominant picture has many positive aspects. Given that this experiment was used in part as a training aid by many laboratories (for example, as a benchmark for inexperienced analysts), full congruence of measurements is unrealistic. Length

measurements by all analysts arranged all samples into their correct ordering in term of annealing level, and the fact that the angular pattern observed by Carlson et al. (1999) and Barbarand et al. (2003a) is now repeated across many laboratories is an encouraging sign of consistency in the community. Also encouraging is that many of the differences among analysts are systematic enough that they can be substantially reduced by normalization with respect to a uniform standard of unannealed induced tracks.

It is important to note that there is no “correct” answer, as there will always be real differences due to etching, microscopy, and analyst decision-making. However, there are “incorrect” answers, which can be recognized as departures from the widely-observed patterns. These took a variety of forms: scatter at all angles (L05-A2, L21-A3, L25-A1, L32-A4); increased observation of short tracks across various angles (L38-A1 samples 1 and 4, 1-L21-A5, L28-A2, L14-A3 samples 2 and 4); scattered or short low-angle tracks (4-L21-A1); out-of-place short high-angle tracks (4-L12-A1).

A very interesting result is how non-influential etching is to the overall patterns in these data. There are no strong tendencies observed that can be traced to etching variations, particularly among the most commonly-employed protocols. This indicates that most variation present is due to the analyst rather than the etching procedure used. We stress, however, that we are not at all diminishing the importance of strict attention to detail when etching; this study was not designed to test the consequences of poor etching procedure.

Recommendations

The two most crucial lessons that arise from the results presented here are the importance of normalization and training. Also of interest is the optimal method for c-axis projection among laboratories that use it. We present below recommendations for each of these.

Normalization

All length measurements should be normalized before interpretation using thermal history inverse modeling, to ensure that they are compatible with the measurements underlying the annealing models. As a minimum step, initial length track should be normalized to Durango apatite, either using sample DUR-2 from this study or an independently-created induced-track sample. However, insofar as initial induced track length is known to vary with apatite chemistry and solubility (Carlson *et al.*, 1999), a more thorough procedure that takes this into account is preferable. The measurable parameter that is best-correlated with initial track length is D_{par} (Carlson *et al.*, 1999). Four methods might thus be considered:

- 1) *Use the DUR-2 measurement as the “initial track length” for modeling software.*

This is at best a first-order correction, as it neglects that Durango apatite actually has a slightly longer initial track length than typical F-apatites (Carlson *et al.*, 1999), which are the most commonly-encountered variety in practice.

- 2) *Adjust length measurements using DUR-2, and use published models for extrapolation.* An adjustment factor for mean length, a_{lm} , based on DUR apatite can be calculated for an analyst as:

$$a_{lm} = \frac{l_{m,DUR,published}}{l_{m,DUR,analyst}} \quad (1)$$

where the numerator is the unannealed induced Durango mean track length measurement underlying the published annealing model calibration (i.e. from Carlson *et al.*, 1999 or Barbarand *et al.*, 2003) and the denominator is a particular analyst's corresponding measurement. Length measurements can be multiplied by this factor before being entered into modeling software, or the software may allow entry of a_{lm} . It carries the advantage of still using etch figures or composition (assuming they are

measured) to better approximate initial length, and leverages the many measurements that underlie the published calibrations. If etch figures are used, they would require a similar adjustment factor:

$$a_{Dpar} = \frac{D_{par,DUR,published}}{D_{par,DUR,analyst}} \quad (2)$$

The primary shortcoming of this solution is that it is based on a single measurement, which provides only limited information on whether there is a change in how length varies among apatites.

- 3) *Use the same method as 2, with more apatite varieties.* Sobel and Seward (2010) advocate a cross-calibration of D_{par} data using two apatite standards, Durango and Fish Canyon, in which the user-measured values are plotted against the published ones, and a line is fitted through them which also passes through the origin. This approach is mathematically equivalent to option 2 above, simply averaging together two or even more apatites, and can be applied equally to length data. Thus:

$$a_{lm} = \frac{\sum l_{m,published}}{\sum l_{m,analyst}} \quad (3)$$

$$a_{Dpar} = \frac{\sum D_{par,published}}{\sum D_{par,analyst}} \quad (4)$$

This approach has the advantage of being less sensitive to a single analysis, and incorporating information from different apatites.

- 4) *Construct complete new calibrations between initial track length and solubility or composition using multiple apatites.* This method would be most rigorous, but also the most demanding, both in terms of effort and the demands placed upon the experimental material. In particular, it would be necessary to have samples spanning

the range of solubility/composition, as well as the variability in the initial track length documented in F-apatites (Carlson et al., 1999).

Figure 9 illustrates normalization methods 1 through 3, using data measured by an analyst for Durango and Fish Canyon standards (DUR $l_m=16.05\pm0.08\ \mu\text{m}$, $D_{par} = 1.98\pm0.03\ \mu\text{m}$; FCT $l_m=16.05\pm0.08\ \mu\text{m}$, $D_{par} = 2.44\pm0.04\ \mu\text{m}$). In this example it is assumed that the analyst has decided that the C99 c-axis projection model is more appropriate, and thus the measurements should be normalized based on Carlson et al. (1999) data. The track length measurements are systematically lower than the corresponding ones from Carlson et al. (1999), but the D_{par} measurements are slightly higher (DUR $l_m=16.21\pm0.08\ \mu\text{m}$, $D_{par} = 1.83\pm0.03\ \mu\text{m}$; FCT $l_m=16.38\pm0.08\ \mu\text{m}$, $D_{par} = 2.43\pm0.04\ \mu\text{m}$). Figure 9 shows the Carlson et al. (1999) l_m and D_{par} data, with apatites DUR and FCT highlighted, along with the published linear fit. The analyst's corresponding measurements are plotted, as well as the linear relationships based on each normalization method. Method 1 provides an invariant line, which is sub-optimal but arguably defensible if only near-end-member F-apatites are being considered. Method 2 captures the variation in initial length documented by Carlson et al. (1999), but with a slightly different slope caused by the 7.6% increase in D_{par} values ($a_{lm} = 1.010$, $a_{Dpar} = 0.924$). When results for FCT apatites are averaged in (method 3), the slope becomes more similar to the published one due to the D_{par} increase being reduced to 3.4%, which is further offset by the l_m decrease of 1.1% ($a_{lm} = 1.011$, $a_{Dpar} = 0.966$).

Of the options discussed, our recommendation is that analysts use method 3, or otherwise method 2 if further annealed standards with induced tracks cannot be obtained. These options leverage the large amount of existing calibration data that underlie the published relationships between initial length and solubility or composition, which makes them more likely to give

reasonable answers when applied to unusual apatite varieties (i.e. large etch figures). Although the difference between methods 2 and 3 is minor in the example shown in Figure 9, we feel that, analogously to age zeta calibration (Hurford, 1990), best practice requires evaluation of multiple standards. The effort required for option 4 is probably only justified if the etching protocol is severely changed, such as by using a weak etchant and/or substantially longer etching times.

A full analysis of the ramifications of neglecting normalization for inverse modeling are beyond the scope of this study, as they are very context-dependent based on the types of samples and geological histories being investigated. Ketcham et al. (2009) showed that omitting normalization affected the shape of the fitted cooling path and the final cooling temperature in cooling-only histories, and the maximum reheating temperature in non-monotonic histories.

C-axis projection

C-axis projection seems to increase inter-laboratory compatibility, and accounts for some differing operator tendencies, particularly at strong levels of annealing. It also removes a substantial component of noise: all tracks at a given level of annealing (i.e. Fig. 5) reflect the same thermal input despite their difference in length, and c-axis projection responds by utilizing, rather than discarding, the information in track angle.

It is worth reconsidering which is the appropriate c-axis projection model for a given analyst or lab group to use. The B03 model seems to represent the majority of the community, but some labs are better represented by C99 model. The spread in Figure 6B indicates that four-point fits are not enough data to make a definitive judgment in any single case, however. The C99 model tends to result in larger $l_{c,mod}$ values, because increased anisotropy means that the lengths of high- ϕ tracks are increased more when being projected to c-axis-parallel. Thus, in Figure 7D-F, the C99 projection model will cause the data for a given lab or analyst to move

rightwards, slightly at low degrees of annealing and more at higher degrees. In some cases this step can increase compatibility among analysts and lab groups; for example, using C99 for lab 13 appears on the whole to increase intercompatibility with other large lab groups (14, 32).

It is in fact possible to create a “tunable” parameter that adjusts the projection model slope+intercept to maximize compatibility among laboratories. However, we are cautious about recommending such a step, as we have not ascertained the reasons underlying this apparent change in the evolution of anisotropy among analysts. The divergent answers in C99 and B03 are both real, as they each reflect dozens of careful experiments, but we don’t yet know what makes them real. Also, again, some divergences observed in this study are likely to be simply a case of inadequate training or attention to detail, and it would be unwise to create a fudge factor to compensate for this rather than addressing the root of the problem.

We thus recommend that each lab evaluate for itself which is the preferable model to employ, using the four samples from this study, or equivalents, to decide which more closely reflects the measurements they produce. The model chosen should be reported when thermal history inversion is used.

Training

In addition to the protocols developed by experienced workers for their respective laboratories, the samples distributed in this study can be a useful training resource. In particular, we recommend a training regimen of measuring these four samples (or equivalents) and critiquing the results, if necessary repeatedly, until they are judged suitably compatible with the community, before measurement and utilization of track lengths for research is undertaken. Results should be evaluated not only for the usual mean and standard deviation but also for

consistent distribution with angle, and careful attention to how borderline cases are evaluated and pitfalls avoided.

These mounts are good for training and inter-laboratory comparison, but not perfect. They are simple length-angle distributions, and after an analyst begins to measure a pattern may be recognized, which can in turn bias further measurements of that sample. Measuring “blind” (i.e. not seeing tables or summaries of measurements as they are made) is thus crucial. The use of megacryst slabs does not test for grain selection, and the plentitude of tracks may shift an analyst’s bias in evaluating track suitability (i.e. borderline cases may be more likely to be passed over). Measurement of the samples in this study also provides no information about relative probability of sampling from different length populations, and whether this tendency varies among analysts. In view of these considerations, samples containing multiple, known annealed populations would be a valuable additional inter-calibration and training tool, and are being created by the lead author.

Implications

The results of this study indicate that there has been some degree of scatter in apatite fission-track length data used for research that can be traced to the human element in their measurement, which in turn is likely to affect some aspects of thermal history inverse modeling. It is also clear that a large component of the problem can be addressed fairly simply and easily through normalizing for length and angle and, where necessary, enhancing training regimens.

The time is approaching when automated systems may take over the measurement of length data, which may enhance or even come close to assuring inter-laboratory consistency. Even over the interval between when most of the measurements in this study were made and the present, there has been considerable progress in using image-analysis-based methods to improve

the picking of track end-points (Donelick et al., 2013; Gleadow and Seiler, 2013). However, full automation of track identification and evaluation is still some time away, with universal acceptance and adoption of these solutions even further in the future. In the intervening time, the measures advocated here should serve to improve the overall quality of length data produced by the fission-track community, and in turn the interpretations generated from those data.

Acknowledgements

Our foremost and deepest thanks go to the many individuals who participated in this study. Constructive reviews by R. Flowers and K. Gallagher improved the manuscript. We also thank the Jackson School of Geosciences for its support of the University of Texas fission-track laboratory, and M. Tamer for helping draft figure 1 and contributing suggestions and additional measurements.

References

- Barbarand, J., Carter, A., Wood, I., and Hurford, A.J. (2003a) Compositional and structural control of fission-track annealing in apatite. *Chemical Geology*, 198, 107-137.
- Barbarand, J., Hurford, A.J., and Carter, A. (2003b) Variation in apatite fission-track length measurement: implications for thermal history modelling. *Chemical Geology (Isotope Geoscience Section)*, 198, 77-106.
- Bhandari, N., Bhat, S.G., Lal, D., Rajagopalan, G., Tamhane, A.S., and Venkatavaradan, V.S. (1971) Fission fragment tracks in apatite: recordable track lengths. *Earth and Planetary Science Letters*, 13, 191-199.
- Burtner, R.L., Nigrini, A., and Donelick, R.A. (1994) Thermochronology of lower Cretaceous source rocks in the Idaho-Wyoming thrust belt. *American Association of Petroleum Geologists Bulletin*, 78(10), 1613-1636.
- Carlson, W.D., Donelick, R.A., and Ketcham, R.A. (1999) Variability of apatite fission-track annealing kinetics I: Experimental results. *American Mineralogist*, 84, 1213-1223.
- Crowley, K.D., Cameron, M., and Schaefer, R.L. (1991) Experimental studies of annealing etched fission tracks in fluorapatite. *Geochimica et Cosmochimica Acta*, 55, 1449-1465.
- Donelick, R.A. (1991) Crystallographic orientation dependence of mean etchable fission track length in apatite: An empirical model and experimental observations. *American Mineralogist*, 76, 83-91.
- Donelick, R.A., Donelick, M.B., O'Sullivan, P.B., McMillan, J., Hourigan, J.K., and Juel, E. (2013) Three-dimensional spatial characteristics and contents of zircon crystals from high resolution optical imagery for the fission track, (U-Th-Sm)/He, and U-Th-Pb systems. *American Geophysical Union Fall Meeting*, p. T42C-06, San Francisco.

- Donelick, R.A., Ketcham, R.A., and Carlson, W.D. (1999) Variability of apatite fission-track annealing kinetics II: Crystallographic orientation effects. *American Mineralogist*, 84, 1224-1234.
- Donelick, R.A., and Miller, D.A. (1990) Enhanced TINT fission track densities in low spontaneous track density apatites using ^{252}Cf -derived fission fragment tracks: A model and experimental observations. *International journal of radiation applications and instrumentation. Part D, Nuclear tracks and radiation measurements*, 18(3), 301-307.
- Donelick, R.A., O'Sullivan, P.B., and Ketcham, R.A. (2005) Apatite fission-track analysis. In P.W. Reiners, and T.A. Ehlers, Eds. *Reviews in Mineralogy and Geochemistry*, 58, p. 49-94.
- Galbraith, R.F. (2005) *Statistics for Fission Track Analysis*. 219 p. Chapman and Hall, Boca Raton.
- Galbraith, R.F., Laslett, G.M., Green, P.F., and Duddy, I.R. (1990) Apatite fission track analysis: geological thermal history analysis based on a three-dimensional random process of linear radiation damage. *Philosophical Transactions of the Royal Society of London A*, 332, 419-438.
- Gallagher, K. (1995) Evolving temperature histories from apatite fission-track data. *Earth and Planetary Science Letters*, 136, 421-435.
- Gallagher, K. (2012) Transdimensional inverse thermal history modeling for quantitative thermochronology. *Journal of Geophysical Research*, 117, B02408.
- Gleadow, A.J.W., Duddy, I.R., Green, P.F., and Lovering, J.F. (1986) Confined fission track lengths in apatite: a diagnostic tool for thermal history analysis. *Contributions to Mineralogy and Petrology*, 94, 405-415.
- Gleadow, A.J.W., and Seiler, C. (2013) Fission track length distributions in multi-system thermochronology. *American Geophysical Union Fall Meeting*, p. T42C-08, San Francisco.
- Green, P.F., Duddy, I.R., Gleadow, A.J.W., Tingate, P.R., and Laslett, G.M. (1986) Thermal annealing of fission tracks in apatite 1. A qualitative description. *Chemical Geology (Isotope Geoscience Section)*, 59, 237-253.
- Green, P.F., Duddy, I.R., Laslett, G.M., Hegarty, K.A., Gleadow, A.J.W., and Lovering, J.F. (1989) Thermal annealing of fission tracks in apatite 4. Quantitative modeling techniques and extension to geological time scales. *Chemical Geology (Isotope Geoscience Section)*, 79, 155-182.
- Green, P.F., and Durrani, S.A. (1977) Annealing studies of tracks in crystals. *Nuclear Track Detection*, 1(1), 33-39.
- Hurford, A.J. (1990) Standardization of fission track dating calibration: Recommendation by the Fission Track Working Group of the I.U.G.S. Subcommittee on Geochronology. *Chemical Geology (Isotope Geoscience Section)*, 80, 171-178.
- Jonckheere, R., Enkelmann, E., Min, M., Trautmann, C., and Ratschbacher, L. (2007) Confined fission tracks in ion-irradiated and step-etched prismatic sections of Durango apatite. *Chemical Geology*, 242, 202-217.
- Jonckheere, R., and Ratschbacher, L. (2010) On measurements of non-horizontal confined fission tracks. In R.W. Brown, Ed. *12th International Conference on thermochronometry*, p. 60, Glasgow.
- Jonckheere, R., and Wagner, G.A. (2000) On the occurrence of anomalous fission tracks in apatite and titanite. *American Mineralogist*, 85, 1744-1753.
- Ketcham, R.A. (2003) Observations on the relationship between crystallographic orientation and biasing in apatite fission-track measurements. *American Mineralogist*, 88, 817-829.
- Ketcham, R.A. (2005) Forward and inverse modeling of low-temperature thermochronometry data. In P.W. Reiners, and T.A. Ehlers, Eds. *Reviews in Mineralogy and Geochemistry*, 58, p. 275-314.
- Ketcham, R.A., Carter, A.C., Donelick, R.A., Barbarand, J., and Hurford, A.J. (2007a) Improved measurement of fission-track annealing in apatite using c-axis projection. *American Mineralogist*, 92, 789-798.
- Ketcham, R.A., Carter, A.C., Donelick, R.A., Barbarand, J., and Hurford, A.J. (2007b) Improved modeling of fission-track annealing in apatite. *American Mineralogist*, 92, 799-810.

- Ketcham, R.A., Donelick, R.A., Balestrieri, M.L., and Zattin, M. (2009) Reproducibility of apatite fission-track length data and thermal history reconstruction. *Earth and Planetary Science Letters*, 284, 504-515.
- Ketcham, R.A., Donelick, R.A., and Carlson, W.D. (1999) Variability of apatite fission-track annealing kinetics III: Extrapolation to geological time scales. *American Mineralogist*, 84, 1235-1255.
- Lal, D., Rajan, R.S., and Tamhane, A.S. (1969) Chemical composition of nuclei of $Z > 22$ in cosmic rays using meteoric minerals as detectors. *Nature*, 221, 33-37.
- Laslett, G.M., and Galbraith, R.F. (1996) Statistical modelling of thermal annealing of fission tracks in apatite. *Geochimica et Cosmochimica Acta*, 60, 5117-5131.
- Laslett, G.M., Green, P.F., Duddy, I.R., and Gleadow, A.J.W. (1987) Thermal annealing of fission tracks in apatite 2. A quantitative analysis. *Chemical Geology (Isotope Geoscience Section)*, 65, 1-13.
- Laslett, G.M., Kendall, W.S., Gleadow, A.J.W., and Duddy, I.R. (1982) Bias in measurement of fission-track length distributions. *Nuclear Tracks and Radiation Measurements*, 6(2/3), 79-85.
- Li, N., Wang, L., Sun, K., Lang, M., Trautmann, C., and Ewing, R.C. (2010) Porous fission fragment tracks in fluorapatite. *Physical Review B*, 82, 144109.
- Miller, D.S., Crowley, K.D., Dokka, R.K., Galbraith, R.F., Kowallis, B.J., and Naeser, C.W. (1993) Results of interlaboratory comparison of fission track ages for 1992 Fission Track Workshop. *Nuclear Tracks and Radiation Measurements*, 21(4), 565-573.
- O'Sullivan, P.B., Donelick, R.A., and Ketcham, R.A. (2004) Etching conditions and fitting ellipses: what constitutes a proper apatite fission-track annealing calibration measurement? In P. Andriessen, Ed. 10th International Conference on Fission Track Dating and Thermochronology, p. Abstract code DV-10-O, Amsterdam.
- Sobel, E.R., and Seward, D. (2010) Influence of etching conditions on apatite fission-track etch pit diameter. *Chemical Geology*, 271, 59-69.
- Yamada, R., Tagami, T., and Nishimura, S. (1995) Confined fission-track length measurement of zircon: assessment of factors affecting the paleotemperature estimate. *Chemical Geology (Isotope Geoscience Section)*, 119, 293-306.

Figure Captions

Figure 1. Photomicrographs of confined fission tracks. Black scale bars are 10 μm , and apatite **c** axis orientations marked with white arrows. (A) Transmitted light image of measurable track at intermediate angle to **c** axis. (B) Reflected light image of track in A. (C) Transmitted light image of tracks at $\sim 25^\circ$ to **c** axis; track 1 is measurable, but track 2 intersects surface. (D) Reflected light image of field of view in C, also showing elongated etch figures indicating **c** axis direction. (E) Reflected light image with track 1 near parallel to **c** axis and track 2 near perpendicular. (F) Reflected light image with **c**-axis-perpendicular track with pinched ends. . Images in (A-F) all obtained with transmitted light. (G) Reflected light image of track that appears shortened due to fluid. (H) Same track after fluid has been removed with acetone wash.

Figure 2. Mean track lengths and errors (1 SE) for unannealed sample DUR-2 versus: (A) lab code; (B) years since being trained in fission-track analysis as of the time study measurements were made; (C) approximate number of fission-track mounts measured per year over the previous 3 years; (D) etching method.

Figure 3. Mean track lengths and errors (1 SE) for annealed samples.

Figure 4. Polar plots of fission-track length measurements of four study samples from an experienced analyst (A-D) and a novice (E-H). Codes refer to sample number (i.e. 1-4 indicates DUR-1 through DUR-4), lab number, and analyst number.

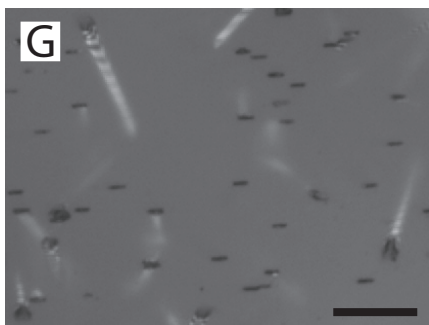
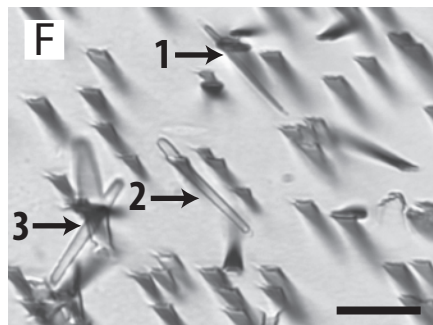
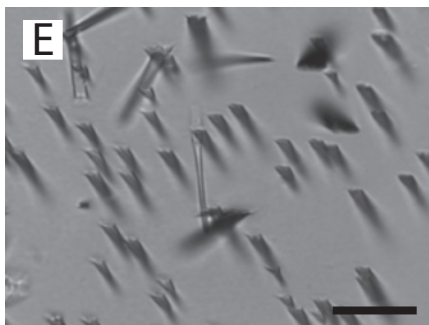
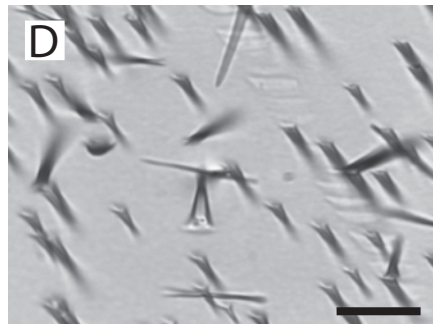
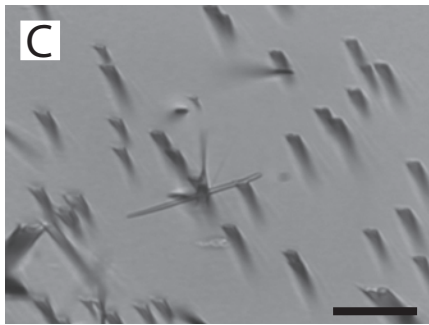
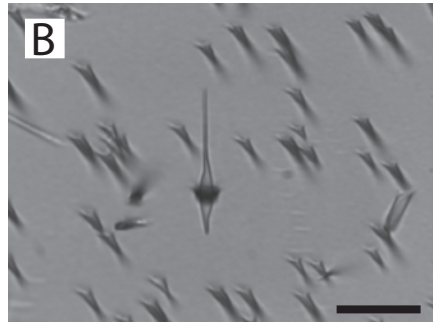
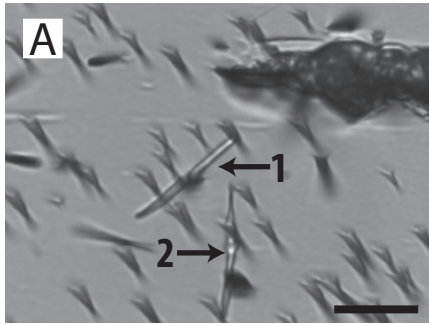
Figure 5. Polar plots of data for six experienced analysts for aliquots of sample DUR-3, showing different tendencies for measuring shortened tracks at high angles to the **c** axis.

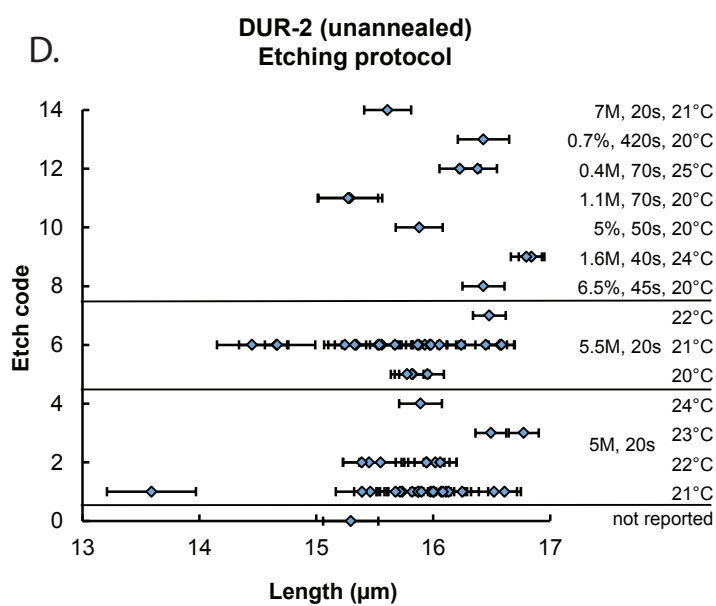
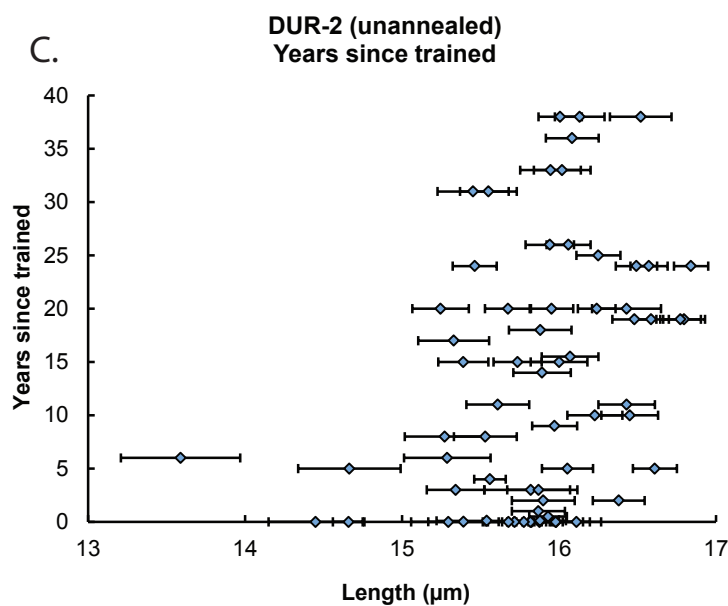
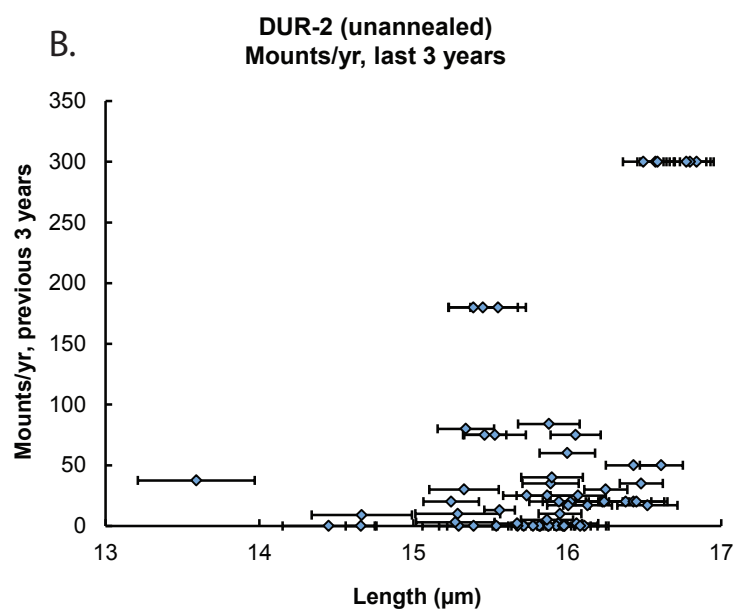
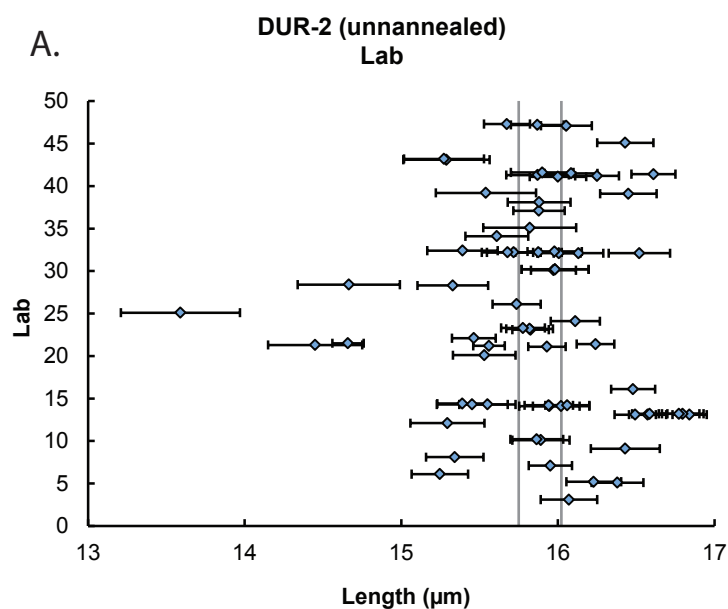
Figure 6. Summary plots showing evolution of track length anisotropy. (A) Individual $l_{c,fit}$ vs. $l_{a,fit}$ data, with lines representing this relationship from Ketcham et al. (2007a) based on data from Carlson et al. (1999) and Barbarand et al. (2003) (C99 and B03, respectively). (B) Slope and intercept of lines fit to four samples for each study participant, and corresponding points from C99 and B03. (C) Range of fitted $l_{c,fit}$ vs. $l_{a,fit}$ slopes for each etching method reported.

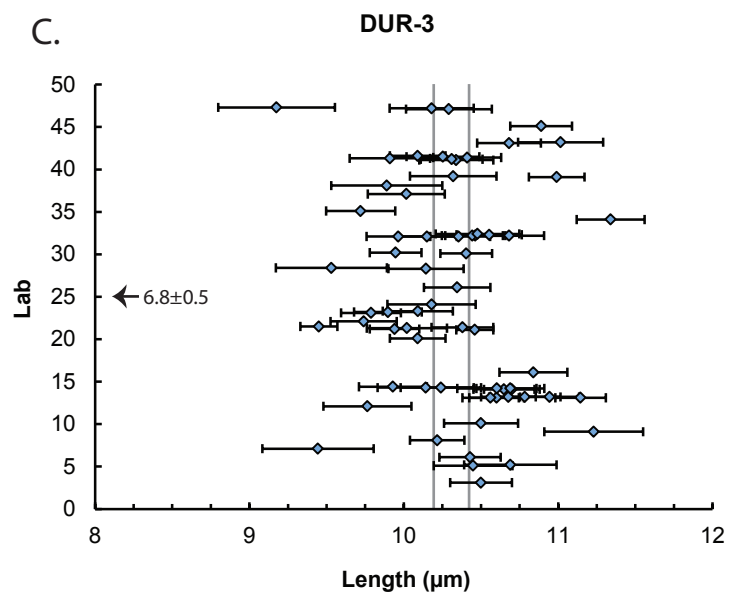
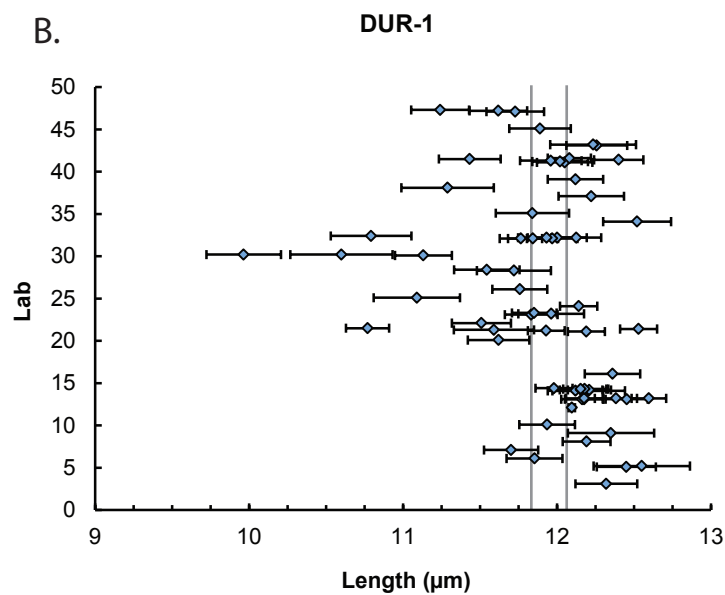
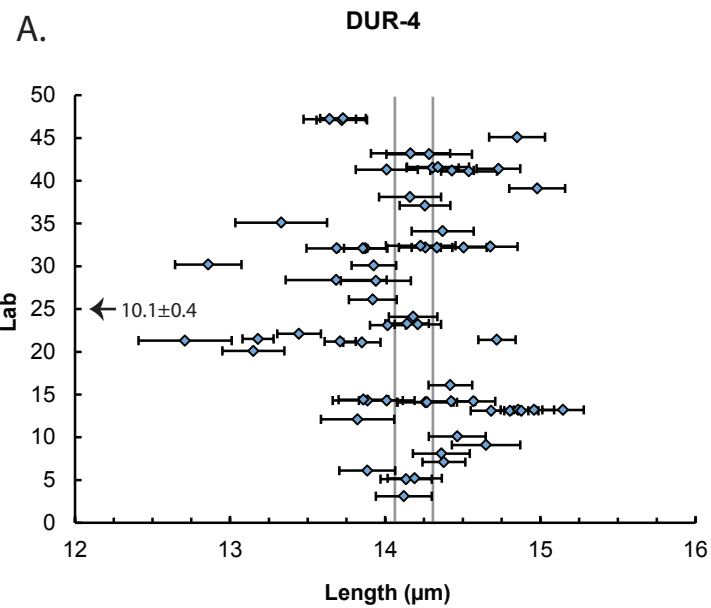
Figure 7. Normalized lengths and errors (1 SE) for annealed samples, for mean (A-C) and c-axis-projected (D-F) data.

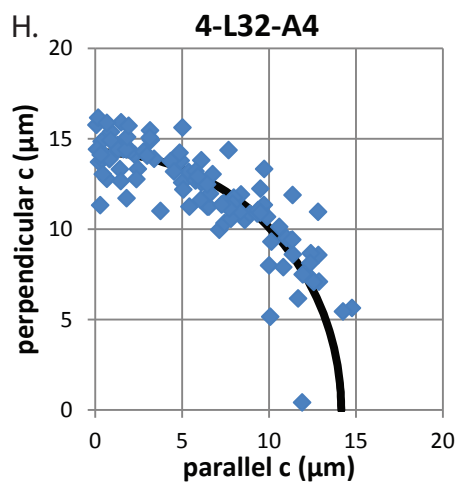
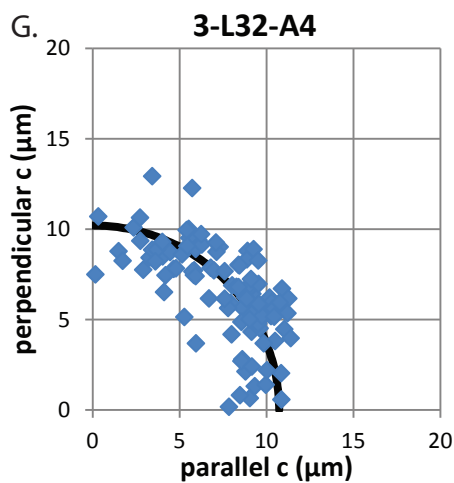
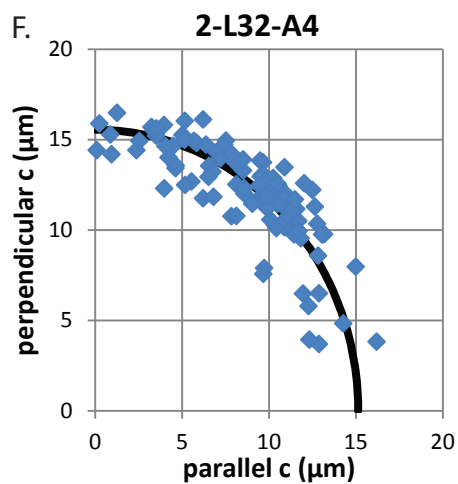
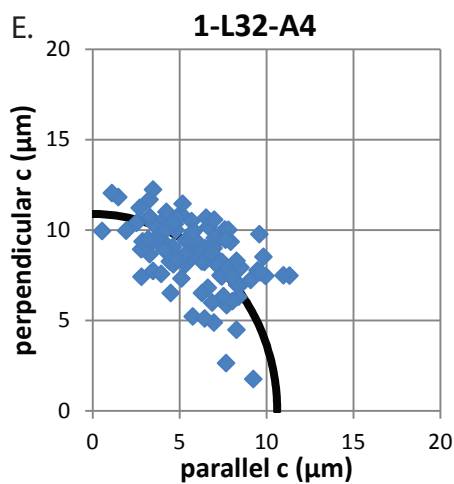
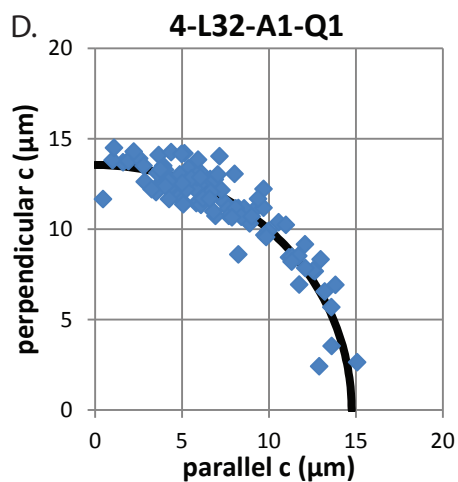
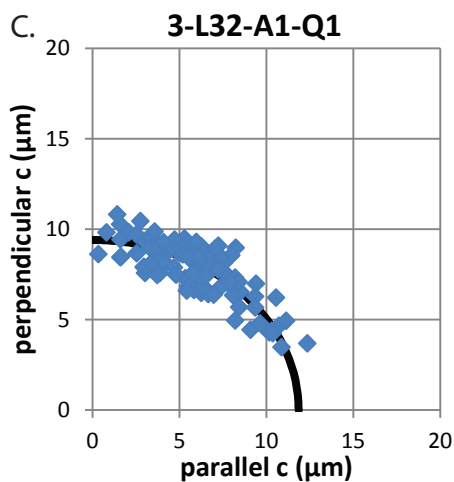
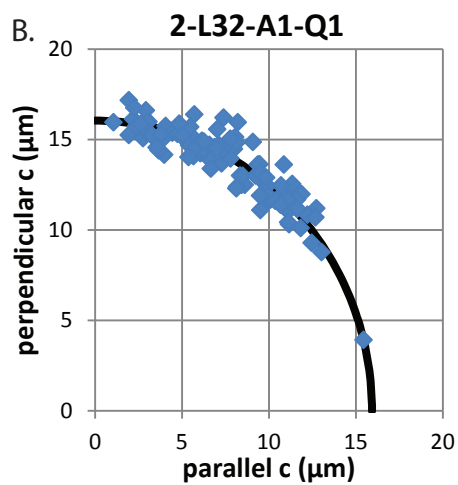
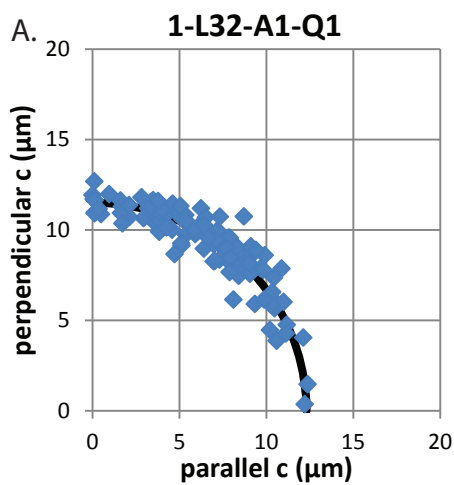
Figure 8. Summary plots of etch figure length (D_{par}) data. (A) Mean D_{par} and error (1 SE) versus lab number. (B) Mean D_{par} and error versus etching method. (C) Normalized D_{par} values for each sample.

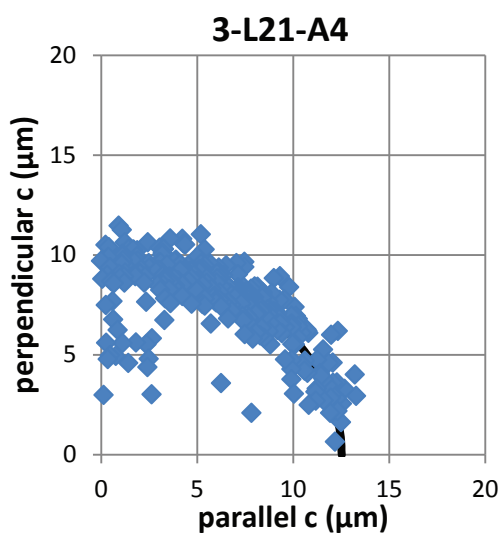
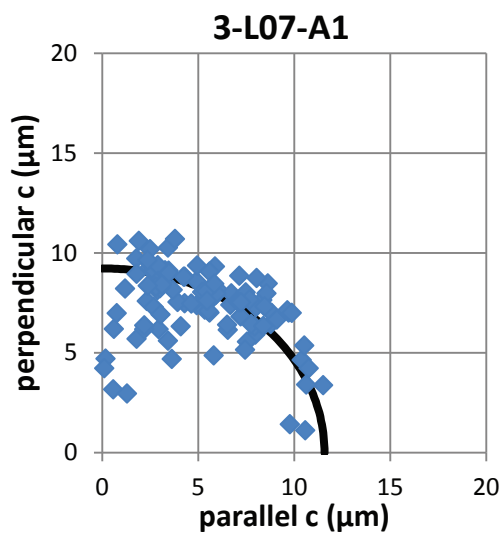
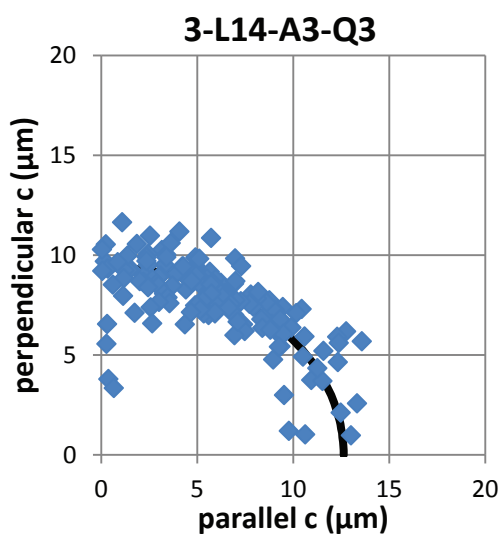
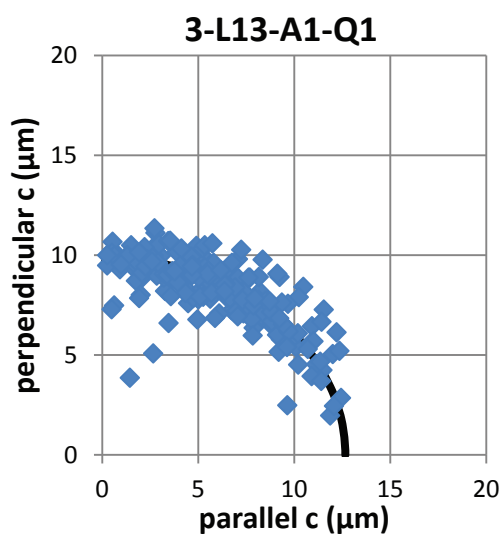
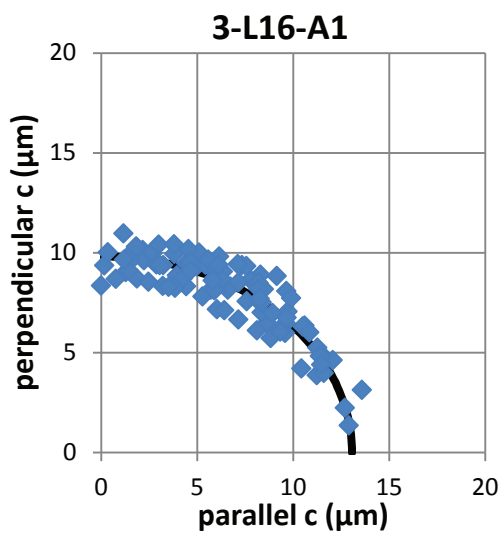
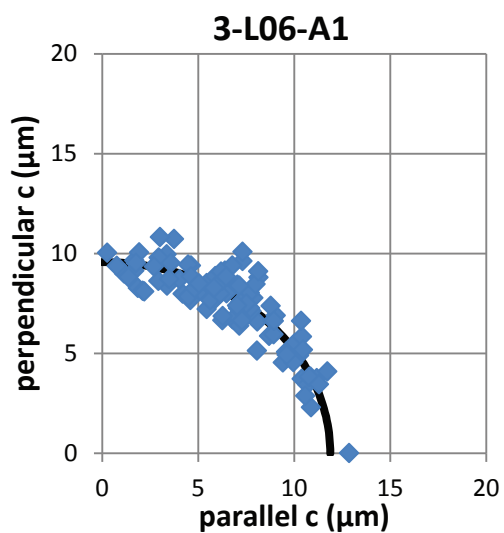
Figure 9. Example showing outcome of three normalization methods for track length and etch figure data discussed in text.

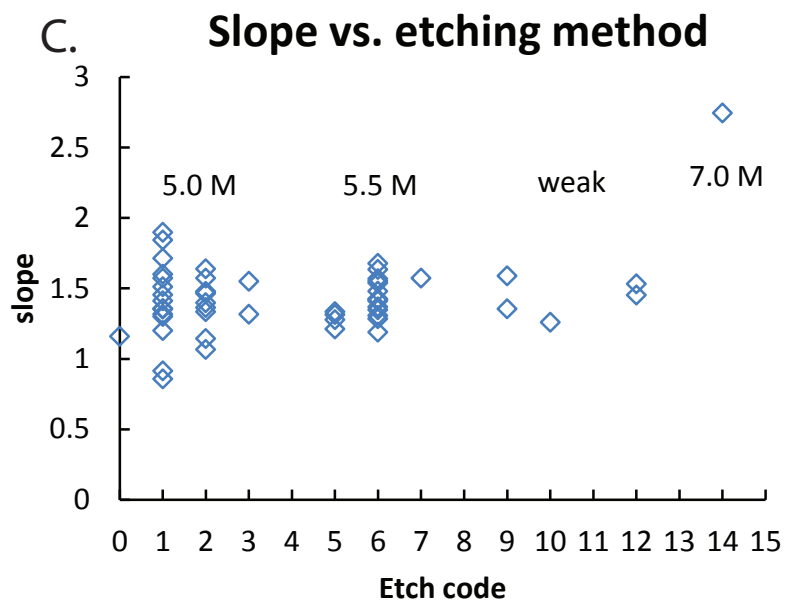
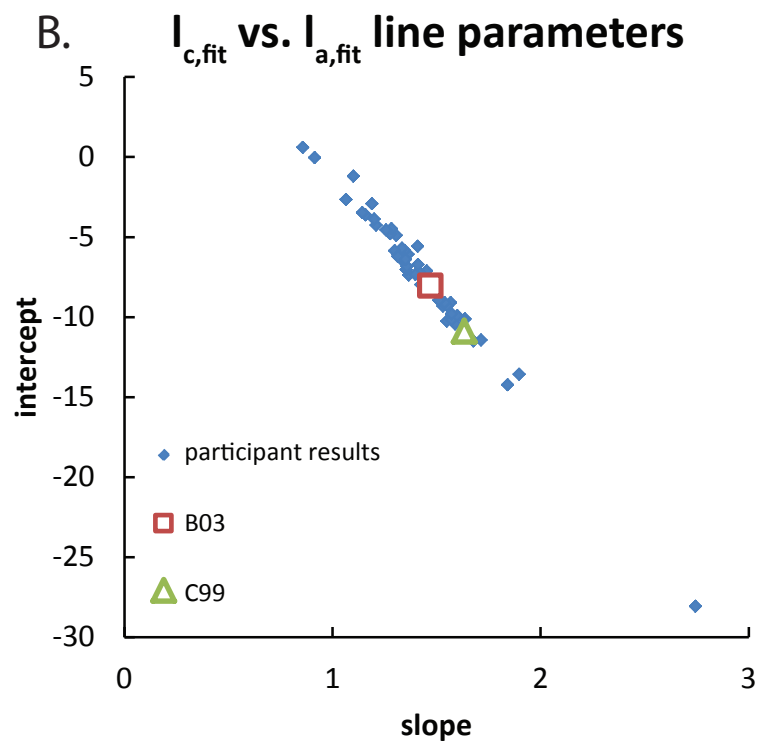
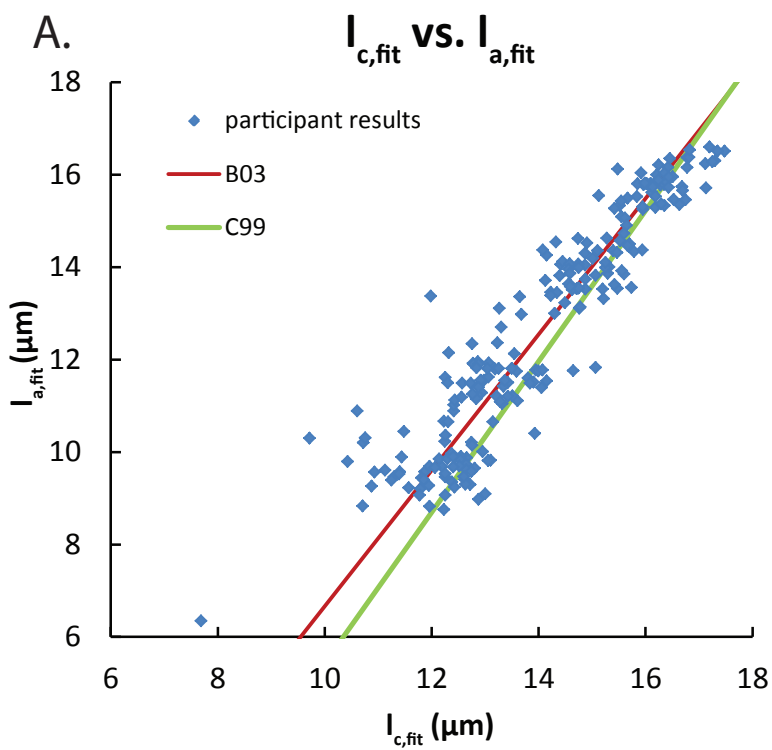


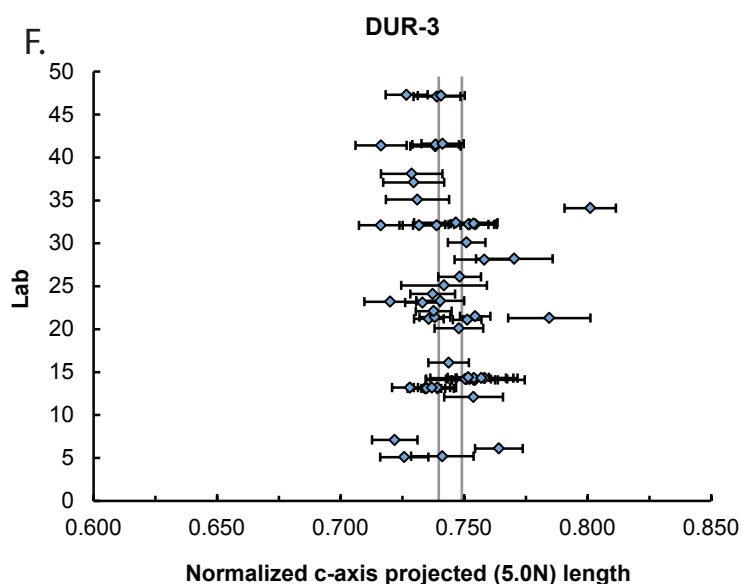
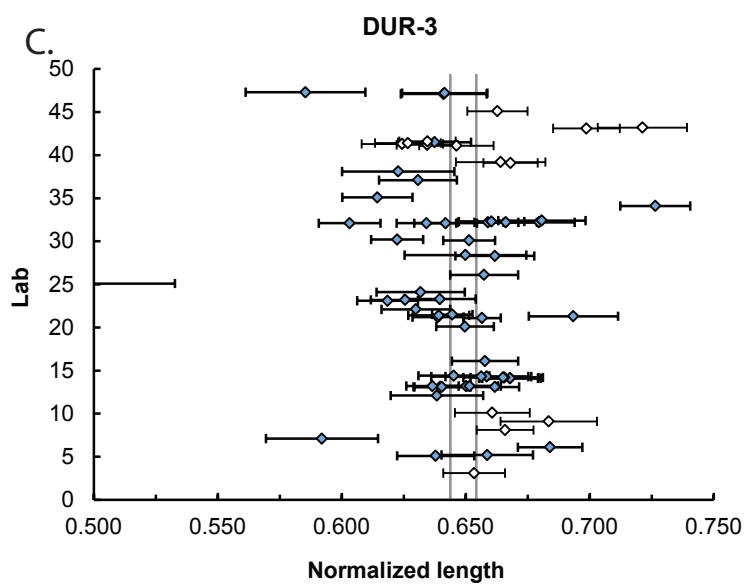
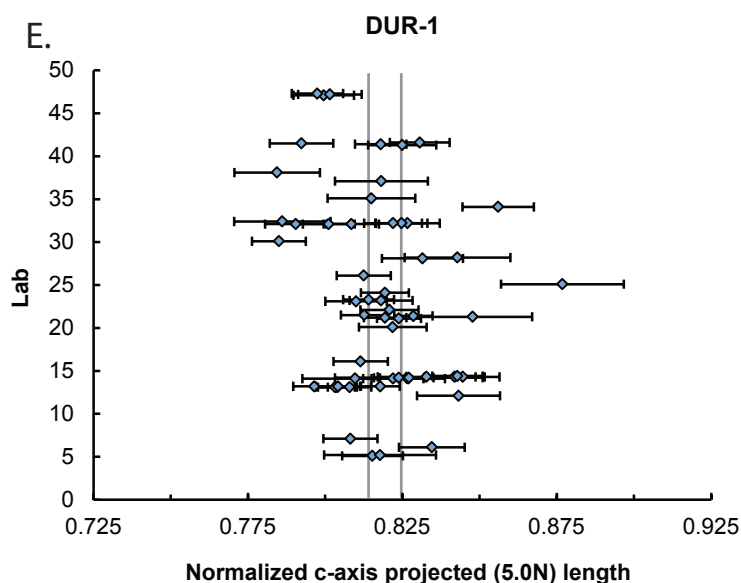
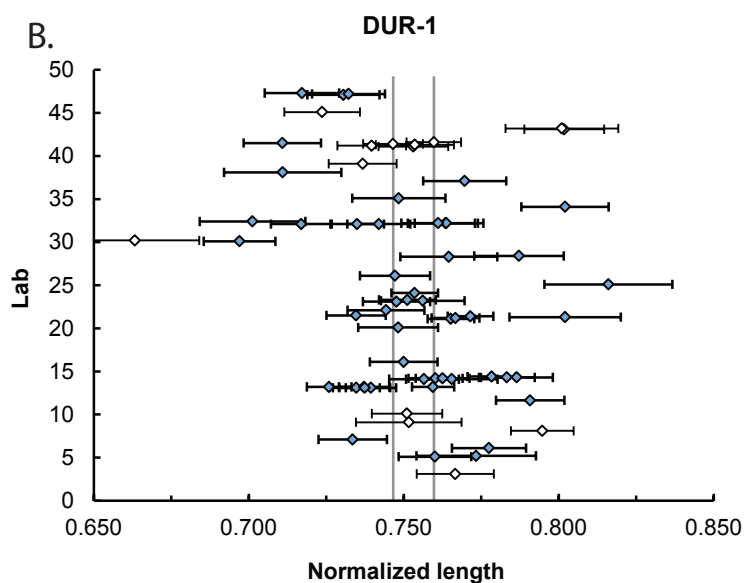
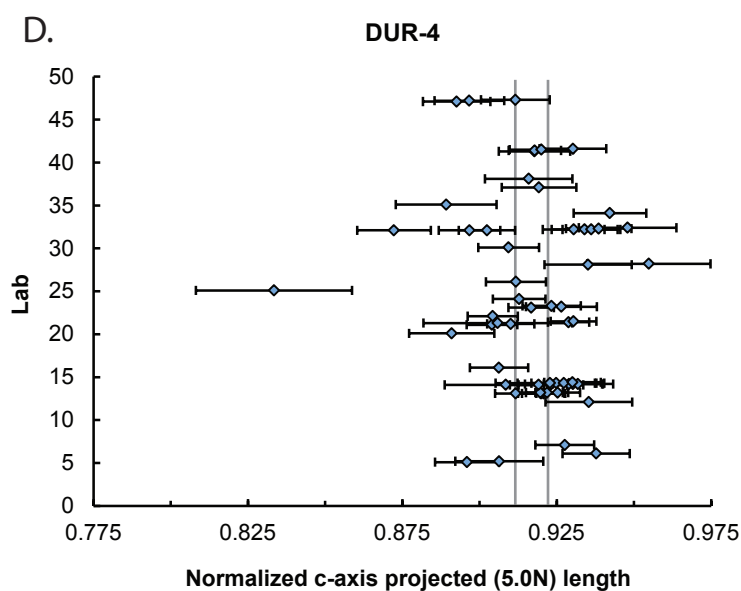
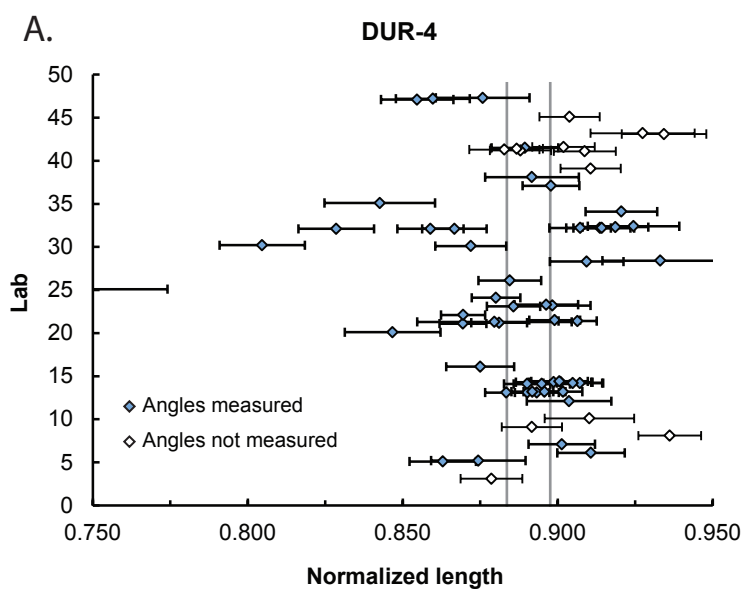


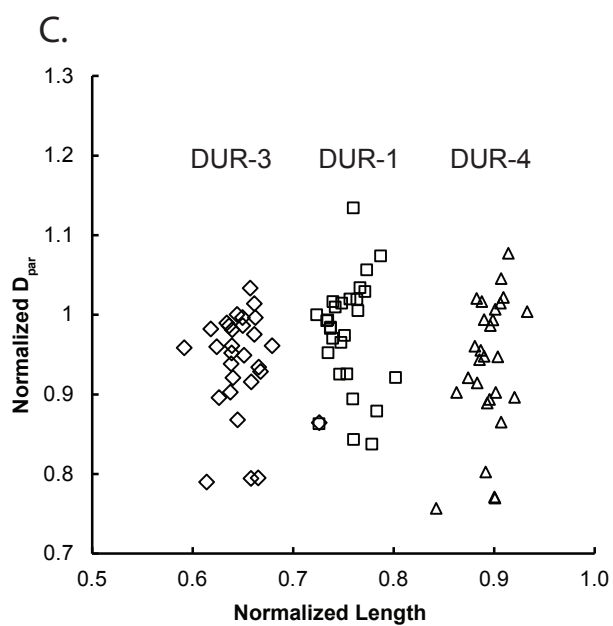
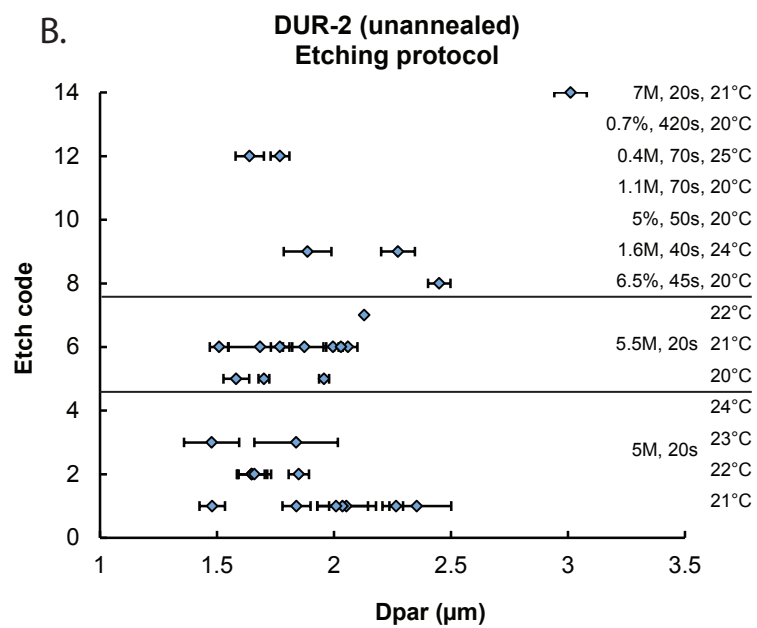
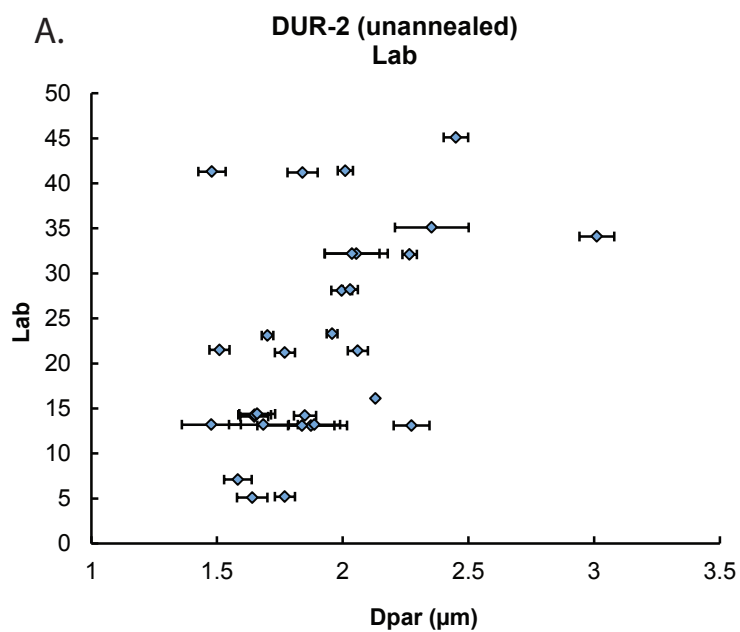












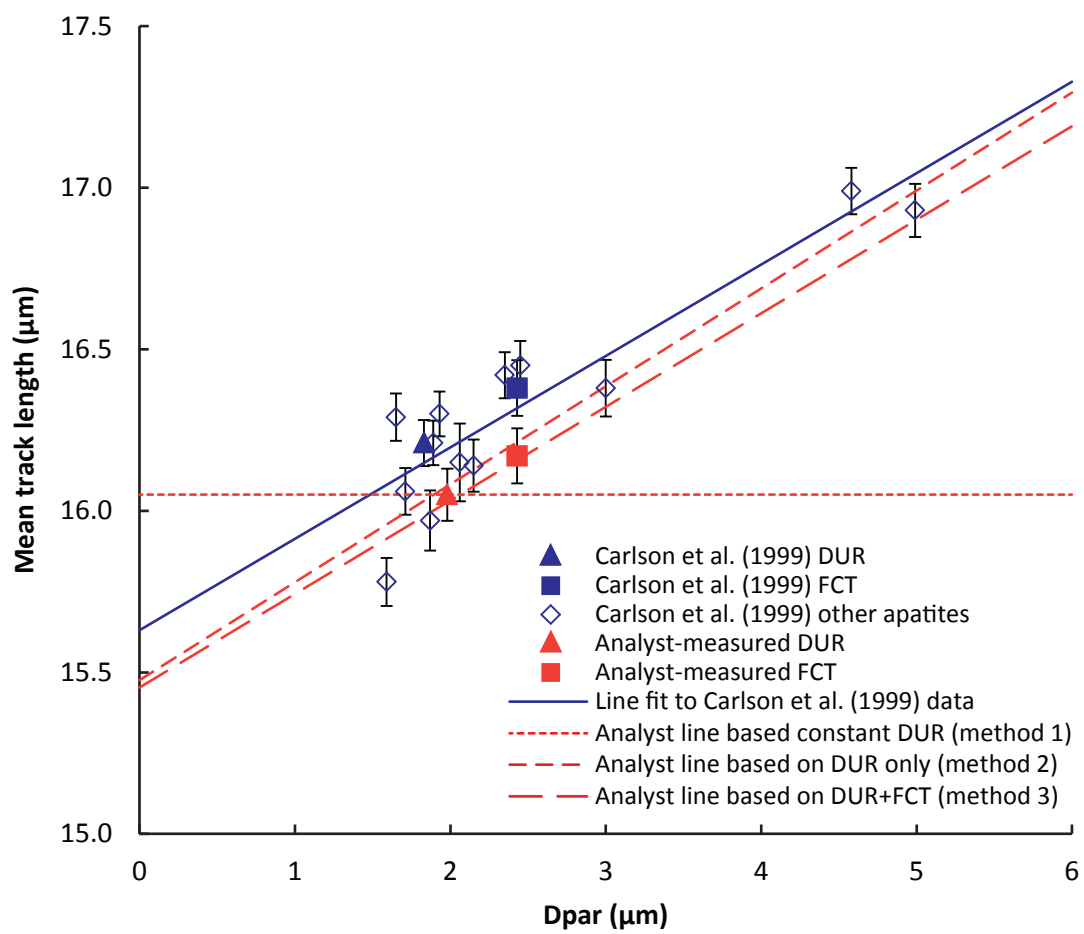


Table 1a: Survey responses for labs and analysts participating in experiment.

Lab ID	Analyst	Etch	Years	M/yr	M/yr (3 yr)	LED	Scope	Mag.	TINCLE used?	System	Standards measured
03	1	1	15.5	25	25	1	1	1600	N	2	N
05	1	12	2	20	20	1	1	1250	N	4	Internal i
	2	12	10	20	20	1	1	1250	N	4	Internal i
06	1	6	20	60	20	1	1	1250	Y	2	N
07	1	5	20	20	10	1	1	1250	?	2	N
08	1	6	3	80	80	?	2	?	N	1	N
09*	1	13	20	20	20	1	1	3840	N	3	DRi+FCi
10	1	4	14	55	35	1	1	1250	Y	2	N
12	1	?	?	?	?	?	?	?	?	?	?
13	1	6, 9, 3	24	300	300	1	1	1563	N	3	DR+FC
	2	6, 9, 3	19	300	300	1	1	1563	N	3	DR+FC
14	1	2	33	20	20	1	1	1250	N+Y	?	N
	2	2	26	2	2	1	1	1250	N+Y	?	N
	3	2	31	180	180	1	1	1250	N+Y	?	N
	4	2	15	180	180	1	1	1250	N	?	N
16	1	7	19	35	35	1	1	1250	N	2	FCs
21	A	6	0.5	2	0	1	1	1250	N	3	N
	B	6	4	15	13	1	1	1250	N	3	N
	C	6	0	0	0	1	1	1250	Y	3	N
	D	6	20	20	20	1	1	1250	N	3	N
	E	6	0	0	0	1	1	1250	Y	3	N
22	1	1	24	75	75	1	1	1600	N	3	Not recently
23	1	5	>1	>1	>1	1	1	100	N	1	DR s+i
	2	5	>1	>1	>1	1	1	100	N	1	DR s+i
	3	5	>1	>1	>1	1	1	100	N	1	DR s+i
24	1	1	>1	few	few	1	1	1000	N	3	Not suitable
25	1	1	6	37.5	37.5	1	1	1250	N	2	N
26	1	1	15	40	25	1	1	1000	N	2	N
28	1	6	17	30	30	1	1	1250	N	2	N
	2	6	5	19	9	1	1	1250	N	2	N
30	1	6	9	10	0	1	1	?	N	2	DRi Pisa
	2	6	0	0	0	2	1	?	N	2	N
32	1	1	38	100	17	1	1	1250	N	2	DR+FC

	2	1	?	?	?	?	1	1250	N	2	DR+FC
	3	1	?	?	?	?	1	1250	N	2	N
	4	1	0.01	0	0	?	1	1250	N	2	N
34	1	14	11	50	?	1	1	1250	N	2	N
35*	1	1	3	0	?	1	1	1250	N	2	N
37	1	6	0.1	0	0	1	1	1000	N	2	N
38	1	10	18	84	84	1	1	1250	N	2	DRi Pisa
39	1	6	10	20	20	1	1	1000	N	2	N
	2	6	0.1	0	0	1	1	1000	N	2	N
41	1	1	15	93	60	1	1	1250	N	2	N
	2	1	25	30	30	1	1	1250	N	2	N
	3	1	3	25	25	1	1	1250	N	2	FCs
	4	1	5	50	50	1	1	1250	N	2	DRs+FCs
	5	1	36	75	0	1	1	1600	N	2	N
	6	1	2	40	40	1	1	1600	N	2	Y
43	1	11	6	15	10	1	1	1500	N	3	DRs+DRi
	2	11	8	3	3	1	1	1500	N	3	N
45	1	8	11	40	50	3	1	1250	N	2	N
47	1	6	5	75	75	1	1	1000	N	1	DR+FC
	2	6	1	15	15	1	1	1000	N	1	DR+FC
	3	6	20	5	2	1	1	1600	N	1	DR

Question marks indicate no response provided.

Etch: Codes given in Table 1b;

Years: Number of years before experiment train in fission-track analysis;

M/yr: Estimated average number of track mounts measured per year over career;

M/yr (3 yrs): Estimated average over 3 years preceding experiment;

LED: 1=LED placed over track tips; 2=LED placed tangential to internal arc of track tips;

3=LED placed on opposite tangents of tip arcs on each end of track;

Scope: 1=air; 2=oil immersion;

Mag.: Scope magnification for measurements

System: 1=Autoscan; 2=FTStage; 3=other (custom system); 4=no computer (manual);

Standards measured: DR=Durango; FC=Fish Canyon; i=induced; s=spontaneous; Pisa=measured only during Ketcham et al. (2009) experiment; Y=yes (no details provided); N=none.

* Labs 9 and 35 experience predominantly or exclusively with zircon rather than apatite.

Table 1b: Etch codes and protocols, as specified by respondents

Etch Code	HNO ₃ (M)	HNO ₃ (%)	Time (s)	Temp (°C)	Notes
1	5		20	21	
2	5		20	22	
3	5		20	23	
4	5		20	24	
5	5.5		20	20	
6	5.5		20	21	
7	5.5		20	22	
8		6.5	45	20	
9	1.6		40	24	
10		5	50	20	
11	1.1		70	20	
12	0.4	2.5	70	25	
13		0.7	Up to 420	20	Variable etch time
14	7		20	21	

Table 4: Data for sample DUR-1.

Lab	Anal.	N _l	l _m (μm)	σ _l (μm)	φ _m (°)	σ _φ (°)	l _{c,fit} (μm)	l _{a,fit} (μm)	σ _e (μm)	l _{c,mod(B03)} (μm)	l _{c,mod(C99)} (μm)	D _{par} (μm)	Notes
03	1	100	12.32(10)	0.95	--	--	--	--	--	--	--	--	
05	1	100	12.45(10)	0.96	50	19	13.59(19)	11.75(12)	0.81	13.50(06)	13.79(06)	1.86(02)	
05	2	100	12.55(16)	1.56	44	23	12.76(14)	12.34(14)	1.56	13.40(14)	13.66(13)	1.87(02)	
06	1	100	11.85(09)	0.91	54	22	12.94(20)	11.28(11)	0.77	13.09(06)	13.43(06)	--	
07	1	100	11.70(09)	0.88	59	16	13.22(29)	11.21(11)	0.76	13.11(06)	13.49(05)	1.57(04)	
08	1	221	12.19(08)	1.16	--	--	--	--	--	--	--	--	
09	1	50	12.35(14)	0.98	--	--	--	--	--	--	--	--	
10	1	100	11.94(09)	0.90	--	--	--	--	--	--	--	--	
12	1	93	12.10(10)	0.98	52	22	12.98(19)	11.55(12)	0.88	13.22(07)	13.54(07)	--	
13	1	210	12.18(06)	0.91	59	17	13.81(19)	11.60(07)	0.74	13.44(04)	13.78(03)	1.79(03)	Etch 6
13	1	201	12.45(07)	0.97	55	19	13.95(15)	11.77(08)	0.77	13.59(04)	13.90(04)	2.21(06)	Etch 9
13	1	204	12.16(07)	0.97	60	15	14.15(23)	11.54(08)	0.81	13.45(04)	13.80(04)	1.81(10)	Etch 3
13	2	200	12.60(06)	0.80	55	16	13.55(18)	12.13(09)	0.73	13.67(04)	13.98(04)	1.51(04)	Etch 6
13	2	200	12.38(07)	0.97	57	16	14.00(19)	11.76(08)	0.82	13.57(04)	13.90(04)	1.86(06)	Etch 9
13	2	200	12.18(06)	0.85	58	15	13.19(20)	11.79(08)	0.80	13.43(04)	13.77(04)	1.27(06)	Etch 3
14	1	74	12.21(12)	1.01	57	19	13.91(29)	11.51(13)	0.83	13.43(08)	13.76(07)	--	TINT
14	1	31	11.93(14)	0.75	62	13	13.43(67)	11.50(20)	0.66	13.31(09)	13.68(08)	--	TINCLE
14	1	105	12.12(09)	0.95	58	17	13.84(27)	11.49(11)	0.78	13.39(06)	13.74(05)	1.56(03)	Combined
14	2	105	12.16(07)	0.71	61	21	12.78(22)	11.92(10)	0.67	13.41(05)	13.75(05)	--	TINT
14	2	13	12.67(26)	0.90	54	22	13.23(53)	12.36(33)	0.86	13.70(18)	13.98(17)	--	TINCLE
14	2	118	12.21(07)	0.75	60	21	12.86(20)	11.96(10)	0.71	13.44(05)	13.78(05)	1.56(03)	Combined
14	3	106	12.15(09)	0.92	59	17	12.79(24)	11.90(11)	0.90	13.40(06)	13.75(06)	--	TINT
14	3	46	12.26(12)	0.80	59	19	13.07(35)	11.92(17)	0.74	13.47(08)	13.80(08)	--	TINCLE
14	3	152	12.18(07)	0.88	59	18	12.88(20)	11.90(09)	0.85	13.42(05)	13.76(05)	1.45(05)	Combined
14	4	150	11.98(06)	0.77	61	17	13.06(23)	11.62(09)	0.70	13.32(04)	13.68(04)	1.39(04)	
16	1	100	12.36(09)	0.90	56	19	13.50(22)	11.81(11)	0.78	13.50(06)	13.82(05)	2.12(00)	

20	1	98	11.62(10)	0.97	62	14	13.61(41)	11.11(11)	0.87	13.10(06)	13.50(06)	--	
21	A	252	12.19(06)	0.88	53	18	12.84(13)	11.82(08)	0.84	13.33(04)	13.65(04)	--	
21	B	208	11.93(06)	0.91	48	20	12.86(12)	11.23(09)	0.77	13.03(04)	13.35(04)	1.83(02)	
21	C	125	11.59(13)	1.49	46	23	12.42(14)	10.89(11)	1.41	12.73(10)	13.06(10)	--	
21	D	268	12.53(06)	1.01	54	21	14.08(13)	11.77(07)	0.76	13.63(04)	13.93(03)	2.12(04)	
21	E	259	10.77(07)	1.06	57	17	11.48(15)	10.44(07)	1.03	12.37(05)	12.81(04)	1.50(02)	
22	1	100	11.51(10)	0.95	64	17	12.83(33)	11.15(11)	0.89	13.03(06)	13.43(06)	--	
23	1	100	11.83(09)	0.85	55	18	12.25(22)	11.62(12)	0.84	13.09(07)	13.44(07)	1.64(01)	
23	2	100	11.96(11)	1.06	54	20	13.51(22)	11.21(11)	0.84	13.20(07)	13.53(06)	--	
23	3	100	11.85(07)	0.72	55	19	12.57(21)	11.49(12)	0.66	13.10(05)	13.45(05)	1.91(01)	
24	1	112	12.14(06)	0.64	59	16	13.04(26)	11.81(11)	0.58	13.41(04)	13.75(04)	--	
25	1	100	11.09(14)	1.36	59	19	12.23(26)	10.67(11)	1.31	12.69(08)	13.12(07)	--	
26	1	100	11.76(09)	0.89	55	17	13.32(26)	11.05(12)	0.71	13.06(05)	13.42(05)	--	
28	3	100	11.72(12)	1.08	57	18	13.28(26)	11.09(11)	0.94	13.07(07)	13.44(06)	2.01(02)	
28	4	100	11.54(11)	1.06	52	23	12.42(17)	11.02(11)	0.96	12.81(07)	13.16(07)	2.18(02)	
30	1	108	11.13(09)	0.96	63	14	13.15(40)	10.65(10)	0.84	12.77(06)	13.21(05)	--	
30	2	100	9.97(12)	1.21	63	11	9.00(30)	10.31(15)	1.19	12.06(08)	12.59(07)	--	
0	2	30	10.60(17)	0.91	64	13	12.76(95)	10.15(20)	0.81	12.41(10)	12.90(09)	--	
	(repeat)												
32	1	103	11.77(07)	0.70	56	20	12.30(21)	11.50(12)	0.67	13.04(05)	13.40(06)	--	aliquot a
32	1	102	11.97(08)	0.83	57	20	12.92(22)	11.56(11)	0.75	13.23(05)	13.58(05)	2.29(03)	aliquot b
32	1	104	11.84(08)	0.82	58	18	12.73(24)	11.49(11)	0.76	13.17(06)	13.53(06)	2.18(03)	aliquot c
32	2	102	12.00(10)	0.97	35	24	13.34(26)	11.42(12)	0.86	13.26(06)	13.61(06)	2.09(05)	aliquot a
32	2	102	12.13(08)	0.82	55	20	13.37(21)	11.55(11)	0.64	13.33(05)	13.66(04)	2.07(05)	aliquot b
32	2	102	11.93(09)	0.94	54	20	13.43(22)	11.21(11)	0.72	13.17(06)	13.51(05)	--	aliquot c
32	3	0	.00(00)	0.00	--	--	--	--	--	--	--	--	
32	4	100	10.79(13)	1.31	56	14	10.61(24)	10.89(15)	1.31	12.40(10)	12.84(09)	--	
34	1	100	12.52(11)	1.06	58	16	14.65(32)	11.76(11)	0.88	13.68(07)	14.01(06)	2.77(03)	
35	1	57	11.84(12)	0.90	60	18	12.88(32)	11.40(15)	0.71	13.14(07)	13.50(07)	2.39(07)	
37	1	50	12.22(11)	0.74	51	30	12.32(19)	12.15(16)	0.74	13.22(11)	13.50(12)	--	
38	1	100	11.29(15)	1.55	51	22	12.31(19)	10.65(12)	1.47	12.68(09)	13.04(09)	--	
39	1	80	12.12(09)	0.90	--	--	--	--	--	--	--	--	
39	0	0	.00(00)	0.00	--	--	--	--	--	--	--	--	
41	1	101	12.05(09)	0.91	--	--	--	--	--	--	--	--	
41	2	125	12.02(09)	1.03	--	--	--	--	--	--	--	1.87(03)	
41	2	125	12.18(08)	0.87	--	--	--	--	--	--	--	--	Cf

[illegible]

Table 2: Data for sample DUR-2.

Lab	Anal.	N _l	l _m (μm)	σ _l (μm)	φ _m (°)	σ _s (°)	l _{c,fit} (μm)	l _{a,fit} (μm)	σ _e (μm)	l _{c,mod(B03)} (μm)	l _{c,mod(C99)} (μm)	D _{par} (μm)	Notes
03	1	100	16.07(09)	0.87	--	--	--	--	--	--	--	--	
05	1	100	16.38(08)	0.82	54	20	16.78(18)	16.16(12)	0.80	16.55(06)	16.63(06)	1.64(03)	
05	2	100	16.23(09)	0.87	45	23	16.24(14)	16.21(14)	0.87	16.39(07)	16.46(07)	1.77(02)	
06	1	100	15.25(09)	0.90	56	18	15.55(21)	15.09(12)	0.89	15.68(07)	15.82(06)	--	
07	1	101	15.95(07)	0.70	54	14	16.28(24)	15.78(14)	0.69	16.22(05)	16.32(05)	1.58(03)	
08	1	211	15.34(09)	1.33	--	--	--	--	--	--	--	--	
09	1	50	16.43(11)	0.75	--	--	--	--	--	--	--	--	
10	1	100	15.89(09)	0.92	--	--	--	--	--	--	--	--	
10	2	100	15.87(08)	0.84	59	16	16.04(26)	15.80(12)	0.84	16.17(06)	16.28(06)	--	Repeat
12	1	100	15.29(12)	1.18	51	23	15.62(16)	15.06(12)	1.17	15.68(09)	15.81(09)	--	
13	1	200	16.57(06)	0.84	59	16	17.30(18)	16.30(08)	0.81	16.72(05)	16.79(04)	1.87(05)	Etch 6
13	1	205	16.84(05)	0.78	55	17	17.48(15)	16.51(09)	0.74	16.92(04)	16.97(04)	2.27(04)	Etch 9
13	1	203	16.49(07)	0.94	58	15	17.12(19)	16.24(09)	0.92	16.65(05)	16.73(05)	1.84(09)	Etch 3
13	2	200	16.59(06)	0.80	57	16	17.25(18)	16.28(09)	0.76	16.72(04)	16.79(04)	1.68(07)	Etch 6
13	2	200	16.80(07)	0.94	56	17	17.20(16)	16.60(09)	0.93	16.87(05)	16.93(05)	1.89(05)	Etch 9
13	2	200	16.77(06)	0.91	57	17	17.35(17)	16.51(09)	0.89	16.86(05)	16.92(05)	1.48(06)	Etch 3
14	1	74	15.95(10)	0.83	59	15	16.35(32)	15.79(14)	0.83	16.24(07)	16.35(07)	--	TINT
14	1	27	16.22(18)	0.89	53	17	17.13(41)	15.71(24)	0.83	16.44(14)	16.52(13)	--	TINCLE
14	1	100	16.02(09)	0.87	58	16	16.68(25)	15.74(12)	0.83	16.29(06)	16.39(06)	1.65(03)	Combined
14	2	88	15.94(08)	0.73	59	14	16.18(30)	15.84(14)	0.72	16.23(06)	16.34(05)	--	TINT
14	2	32	16.38(13)	0.74	61	17	16.46(43)	16.35(20)	0.74	16.56(10)	16.64(09)	--	TINCLE
14	2	120	16.06(07)	0.76	59	14	16.21(25)	16.00(12)	0.75	16.32(05)	16.42(05)	1.85(02)	Combined
14	3	129	15.45(11)	1.28	59	17	15.95(22)	15.25(10)	1.27	15.87(08)	16.01(07)	--	TINT
14	3	41	15.86(16)	1.00	57	18	16.75(38)	15.45(19)	0.95	16.17(12)	16.28(11)	--	TINCLE
14	3	170	15.55(09)	1.23	59	17	16.18(19)	15.29(09)	1.21	15.94(07)	16.07(06)	1.65(03)	Combined
14	4	150	15.39(08)	0.93	57	15	15.51(21)	15.33(11)	0.93	15.80(06)	15.94(05)	1.66(04)	

16	1	100	16.48(07)	0.72	60	17	16.78(24)	16.37(12)	0.71	16.64(05)	16.71(05)	2.13(00)	
20	1	94	15.53(10)	0.92	62	12	15.66(35)	15.49(13)	0.92	15.94(07)	16.08(07)	--	
21	1	232	15.93(06)	0.88	49	21	16.09(11)	15.81(09)	0.88	16.17(05)	16.26(04)	--	
21	2	256	15.56(05)	0.87	51	18	15.94(12)	15.31(08)	0.86	15.90(04)	16.02(04)	1.77(02)	
21	3	125	14.45(15)	1.63	51	20	14.32(15)	14.54(12)	1.63	15.01(12)	15.19(11)	--	
21	4	253	16.24(06)	0.88	58	20	16.42(12)	16.16(07)	0.88	16.45(04)	16.53(04)	2.06(02)	
21	5	308	14.66(05)	0.92	54	19	14.90(11)	14.52(07)	0.91	15.22(04)	15.39(04)	1.51(02)	
22	1	99	15.46(07)	0.69	60	14	15.55(29)	15.43(13)	0.69	15.87(05)	16.01(05)	--	
23	1	100	15.83(06)	0.58	63	13	15.97(34)	15.78(12)	0.58	16.16(04)	16.28(04)	1.70(01)	
23	2	99	15.82(07)	0.74	60	19	15.85(22)	15.81(11)	0.75	16.13(06)	16.24(05)	--	
23	3	100	15.78(07)	0.70	57	18	16.12(21)	15.62(12)	0.68	16.10(05)	16.21(05)	1.96(01)	
24	1	102	16.11(08)	0.79	61	14	16.35(30)	16.03(12)	0.79	16.36(06)	16.46(05)	--	
25	1	100	13.59(19)	1.85	57	16	14.76(27)	13.11(12)	1.81	14.47(13)	14.73(12)	--	
26	1	100	15.74(08)	0.76	57	17	16.18(24)	15.53(12)	0.75	16.07(06)	16.19(05)	--	
28	1	100	15.33(11)	1.13	52	19	15.42(18)	15.27(13)	1.13	15.71(09)	15.84(09)	2.00(02)	
28	2	100	14.67(16)	1.64	54	24	14.74(16)	14.62(11)	1.63	15.20(13)	15.37(12)	2.03(01)	
30	1	101	15.97(07)	0.72	62	14	16.39(30)	15.84(11)	0.71	16.27(05)	16.38(05)	--	
30	2	104	15.98(11)	1.09	64	12	15.48(33)	16.12(12)	1.09	16.28(08)	16.39(07)	--	
32	1	101	16.01(07)	0.70	61	14	15.92(29)	16.04(13)	0.69	16.28(05)	16.39(05)	--	Aliquot a
32	1	103	16.13(08)	0.81	57	18	16.51(21)	15.96(11)	0.79	16.37(06)	16.46(06)	2.27(01)	Aliquot b
32	1	104	16.52(10)	0.99	57	18	16.82(21)	16.38(12)	0.98	16.66(07)	16.73(07)	--	Aliquot c
32	2	102	15.72(09)	0.87	53	19	16.35(19)	15.33(12)	0.82	16.04(06)	16.15(06)	2.05(06)	Aliquot a
32	2	103	15.88(07)	0.75	56	19	16.01(20)	15.81(12)	0.74	16.16(06)	16.27(05)	--	Aliquot b
32	2	102	15.68(08)	0.83	55	19	16.30(20)	15.37(12)	0.79	16.02(06)	16.14(06)	2.04(05)	Aliquot c
32	3	100	15.98(09)	0.86	62	16	16.24(26)	15.89(11)	0.86	16.27(07)	16.37(06)	--	
32	4	100	15.39(11)	1.12	55	17	15.13(21)	15.54(14)	1.12	15.77(09)	15.90(09)	--	
34	1	100	15.61(10)	0.96	59	16	15.84(25)	15.53(12)	0.96	15.99(07)	16.11(07)	3.01(03)	
35	1	56	15.82(15)	1.11	53	19	16.63(27)	15.35(17)	1.05	16.13(11)	16.24(10)	2.35(07)	
37	1	50	15.88(08)	0.57	55	23	16.09(24)	15.77(16)	0.56	16.16(06)	16.26(06)	--	

38	1	100	15.88(10)	0.97	56	21	16.14(19)	15.73(12)	0.97	16.16(08)	16.26(07)	--	
39	1	80	16.45(09)	0.80	--	--	--	--	--	--	--	--	
39	2	47	15.54(16)	1.42	--	--	--	--	--	--	--	--	
41	1	100	16.00(09)	0.88	--	--	--	--	--	--	--	--	
41	2	100	16.25(07)	0.70	--	--	--	--	--	--	--	1.84(03)	
41	3	100	15.87(10)	1.01	57	15	15.99(25)	15.82(13)	1.01	16.17(08)	16.28(07)	1.48(03)	
41	4	100	16.61(07)	0.75	61	12	16.82(35)	16.54(13)	0.74	16.73(06)	16.81(05)	2.01(02)	
41	5	100	16.08(08)	0.84	59	13	16.44(30)	15.95(13)	0.83	16.34(06)	16.44(06)	--	Cf
41	6	100	15.90(10)	1.00	61	10	16.43(41)	15.73(15)	0.99	16.21(07)	16.33(07)	--	
43	1	100	15.29(14)	1.37	--	--	--	--	--	--	--	--	
43	2	99	15.27(13)	1.26	--	--	--	--	--	--	--	--	
45	1	100	16.43(09)	0.93	--	--	--	--	--	--	--	2.45(02)	
47	1	100	16.05(08)	0.81	53	22	16.70(18)	15.66(12)	0.75	16.30(06)	16.40(06)	--	
47	2	100	15.87(08)	0.84	53	22	16.53(18)	15.47(12)	0.78	16.16(07)	16.26(06)	--	
47	3	104	15.67(07)	0.75	56	18	16.05(21)	15.49(12)	0.74	16.02(05)	16.14(05)	--	

Table 5: Data for sample DUR-3.

Lab	Anal.	N _l	l _m (μm)	σ _l (μm)	φ _m (°)	σ _e (°)	N _{ell}	l _{c,fit} (μm)	l _{a,fit} (μm)	σ _e (μm)	l _{c,mod(B03)} (μm)	l _{c,mod(C99)} (μm)	D _{par} (μm)	Notes
03	1	100	10.50(10)	0.97	--	--	--	--	--	--	--	--	--	
05	1	100	10.45(13)	1.27	48	18	99	12.38(21)	9.35(12)	0.91	12.02(07)	12.46(06)	1.48(02)	
05	2	100	10.69(15)	1.50	47	21	99	12.19(18)	9.68(12)	1.21	12.16(09)	12.56(08)	1.62(02)	
06	1	100	10.43(10)	0.99	50	16	100	11.87(21)	9.57(12)	0.78	11.98(05)	12.43(05)	--	
07	1	102	9.44(18)	1.82	56	18	90	11.57(27)	9.23(12)	0.97	11.81(06)	12.30(06)	1.52(02)	
08	1	234	10.22(09)	1.35	--	--	--	--	--	--	--	--	--	
09	1	50	11.23(16)	1.13	--	--	--	--	--	--	--	--	--	
10	1	100	10.50(12)	1.18	--	--	--	--	--	--	--	--	--	
12	1	99	9.76(14)	1.42	57	19	93	11.30(26)	9.46(12)	0.91	11.86(06)	12.37(06)	--	
13	1	204	10.60(09)	1.27	55	18	199	12.65(18)	9.87(08)	0.83	12.30(04)	12.75(04)	1.84(03)	Etch 6
13	1	204	11.14(08)	1.17	49	19	203	12.74(14)	10.21(08)	0.86	12.51(05)	12.89(04)	2.22(02)	Etch 9
13	1	200	10.56(09)	1.29	54	17	199	12.80(20)	9.65(08)	1.04	12.24(05)	12.69(05)	1.69(13)	Etch 3
13	2	200	10.78(12)	1.63	51	18	194	13.11(18)	9.82(08)	0.98	12.40(05)	12.82(05)	1.66(04)	Etch 6
13	2	200	10.94(10)	1.36	51	18	196	12.95(17)	10.01(08)	0.93	12.46(05)	12.87(04)	1.79(06)	Etch 9
13	2	175	10.68(09)	1.17	53	15	173	12.55(22)	9.91(09)	0.89	12.29(05)	12.73(04)	1.46(07)	Etch 3
14	1	118	10.65(10)	1.07	54	17	117	12.43(23)	9.89(11)	0.78	12.26(05)	12.70(05)	--	TINT
14	1	34	10.89(21)	1.19	56	19	34	12.25(38)	10.23(20)	1.05	12.40(13)	12.83(12)	--	TINCLE
14	1	152	10.70(09)	1.10	54	18	151	12.38(20)	9.97(09)	0.85	12.29(05)	12.73(05)	1.42(03)	Combined
14	2	85	10.60(13)	1.18	52	17	84	12.65(29)	9.73(13)	0.67	12.22(05)	12.66(05)	--	TINT
14	2	17	11.12(22)	0.89	50	22	17	12.26(41)	10.36(28)	0.64	12.44(11)	12.81(11)	--	TINCLE
14	2	102	10.69(11)	1.15	52	18	101	12.53(23)	9.84(12)	0.68	12.26(05)	12.69(04)	1.47(03)	Combined
14	3	119	10.14(16)	1.70	55	20	115	12.72(23)	9.29(10)	1.03	12.07(07)	12.54(06)	--	TINT
14	3	34	10.57(19)	1.09	55	20	34	12.14(41)	9.85(19)	0.94	12.19(11)	12.64(10)	--	TINCLE
14	3	153	10.24(13)	1.59	55	20	149	12.62(20)	9.41(09)	1.02	12.10(06)	12.56(05)	1.31(04)	Combined
14	4	150	9.93(11)	1.30	56	16	147	11.95(26)	9.27(09)	0.96	11.90(05)	12.41(04)	1.44(04)	
16	1	100	10.84(11)	1.14	53	20	100	13.06(24)	9.82(11)	0.74	12.38(06)	12.80(05)	--	

20	1	84	10.09(09)	0.86	56	13	84	11.40(38)	9.57(14)	0.79	11.92(06)	12.43(05)	--	
21	A	277	10.46(06)	0.96	55	15	277	12.65(20)	9.62(07)	0.73	12.15(03)	12.62(03)	--	
21	B	232	9.94(08)	1.25	49	19	231	11.96(14)	8.82(07)	0.84	11.70(04)	12.18(03)	--	
21	C	125	10.02(13)	1.46	51	23	123	11.25(16)	9.40(10)	1.25	11.82(08)	12.28(08)	--	
21	D	278	10.38(10)	1.69	53	21	262	12.52(13)	9.69(07)	0.86	12.22(04)	12.65(03)	--	
21	E	276	9.45(06)	1.01	54	19	276	10.71(13)	8.83(07)	0.87	11.48(04)	12.01(04)	--	
22	1	101	9.74(11)	1.07	54	16	101	12.23(33)	8.76(11)	0.78	11.71(04)	12.23(04)	--	
23	1	100	9.79(10)	0.96	60	14	100	11.79(41)	9.21(11)	0.84	11.85(05)	12.39(04)	1.67(01)	
23	2	100	9.90(11)	1.09	50	21	100	10.88(18)	9.26(12)	0.98	11.61(07)	12.08(08)	--	
23	3	100	10.09(11)	1.13	55	18	100	11.39(24)	9.52(11)	1.02	11.92(07)	12.41(06)	1.88(01)	
24	1	104	10.18(14)	1.46	63	26	97	12.74(31)	9.58(11)	0.71	12.15(05)	12.62(05)	--	
25	1	50	6.78(23)	1.64	53	16	50	7.69(40)	6.35(18)	1.61	10.74(08)	11.31(08)	--	
26	1	100	10.35(11)	1.07	54	20	100	12.25(23)	9.46(11)	0.77	12.02(05)	12.49(05)	--	
28	1	100	10.14(12)	1.22	54	21	98	11.81(21)	9.44(11)	0.86	11.93(06)	12.40(06)	2.02(02)	
28	2	100	9.53(18)	1.80	54	21	90	11.77(23)	9.07(12)	0.98	11.80(07)	12.29(06)	2.02(02)	
30	1	107	10.40(08)	0.86	60	14	107	12.30(41)	9.86(11)	0.75	12.22(05)	12.71(04)	--	
30	2	100	9.95(08)	0.85	61	13	100	10.43(38)	9.79(13)	0.84	11.95(06)	12.48(05)	--	
32	1	103	10.15(10)	0.98	54	16	103	11.85(28)	9.40(12)	0.80	11.91(05)	12.40(05)	2.23(03)	aliquot a
32	1	102	10.36(10)	1.03	57	19	102	11.44(23)	9.89(11)	0.94	12.10(06)	12.57(06)	--	aliquot b
32	1	101	9.97(10)	1.03	59	15	101	12.43(37)	9.24(11)	0.82	11.93(05)	12.46(04)	--	aliquot c
32	2	103	10.68(11)	1.15	31	25	103	11.96(16)	9.69(12)	0.87	12.06(06)	12.46(06)	1.97(06)	aliquot a
32	2	106	10.46(10)	1.00	55	17	106	12.40(26)	9.68(11)	0.75	12.15(05)	12.61(04)	2.06(06)	aliquot b
32	2	102	10.44(10)	1.00	53	18	102	12.06(23)	9.66(11)	0.78	12.09(05)	12.55(05)	1.90(04)	aliquot c
32	3	117	10.55(11)	1.14	57	19	116	12.40(23)	9.90(10)	0.87	12.27(06)	12.74(05)	--	
32	4	100	10.48(14)	1.35	42	20	100	10.72(14)	10.20(15)	1.34	11.78(11)	12.16(12)	--	
34	1	100	11.34(11)	1.13	57	18	100	13.93(28)	10.40(10)	0.73	12.81(06)	13.20(05)	2.60(04)	
35	1	101	9.72(11)	1.93	53	19	93	12.25(24)	9.07(12)	0.94	11.88(06)	12.35(06)	1.86(05)	
37	1	50	10.02(12)	0.87	54	20	50	10.93(30)	9.56(16)	0.79	11.79(09)	12.28(09)	--	
38	1	100	9.89(18)	1.76	52	23	94	11.13(18)	9.61(12)	1.12	11.85(08)	12.30(08)	--	
39	1	80	10.99(09)	0.85	--	--	--	--	--	--	--	--	--	

39	2	50	10.32(14)	1.25	--	--	--	--	--	--	--	--	--	
41	1	101	10.34(12)	1.23	--	--	--	--	--	--	--	--	--	
41	2	105	10.31(10)	1.02	--	--	--	--	--	--	--	--	1.82(03)	
41	3	100	9.91(13)	1.26	59	14	98	12.63(52)	9.30(12)	0.83	11.98(05)	12.51(04)	1.42(02)	
41	4	100	10.41(11)	1.05	51	18	98	10.76(19)	10.31(14)	0.86	12.01(08)	12.45(08)	1.80(02)	
41	5	100	10.25(12)	1.17	56	16	99	12.25(32)	9.53(12)	0.95	12.07(06)	12.56(06)	--	Cf
41	6	101	10.09(09)	0.89	59	11	100	12.60(55)	9.47(13)	0.66	12.03(04)	12.54(04)	--	
43	1	96	10.68(10)	1.00	--	--	--	--	--	--	--	--	--	
43	2	95	11.02(14)	1.33	--	--	--	--	--	--	--	--	--	
45	1	100	10.89(10)	1.00	--	--	--	--	--	--	--	--	2.44(07)	
47	1	100	10.29(14)	1.39	53	20	100	13.01(25)	9.09(10)	0.92	12.05(06)	12.52(05)	--	
47	2	100	10.18(14)	1.36	53	20	100	12.87(25)	8.97(10)	0.88	11.97(06)	12.44(05)	--	
47	3	111	9.18(19)	1.99	57	18	96	12.08(28)	8.88(11)	0.90	11.64(06)	12.17(05)	--	

Table 3: Data for sample DUR-4.

Lab	Anal.	N _l	l _m μm	σ _l μm	φ _m °	σ _φ °	l _{c,fit} μm	l _{a,fit} μm	σ _e μm	l _{c,mod(B03)} μm	l _{c,mod(C99)} μm	D _{par} μm	Notes
03	1	100	14.12(08)	0.80	--	--	--	--	--	--	--	--	
05	1	100	14.13(09)	0.88	53	17	14.88(21)	13.74(12)	0.82	14.83(06)	15.03(06)	1.48(02)	
05	2	100	14.19(12)	1.24	53	17	14.42(20)	14.06(13)	1.23	14.85(10)	15.05(09)	1.63(02)	
06	1	100	13.89(08)	0.83	60	19	14.87(25)	13.52(11)	0.76	14.71(06)	14.94(05)	--	
07	1	105	14.38(09)	0.88	56	14	15.60(30)	13.85(13)	0.81	15.05(06)	15.25(05)	1.59(02)	
08	1	175	14.36(08)	1.03	--	--	--	--	--	--	--	--	
09	1	50	14.65(08)	0.60	--	--	--	--	--	--	--	--	
10	1	100	14.46(11)	1.15	--	--	--	--	--	--	--	--	
12	1	100	13.82(10)	1.04	60	18	15.22(25)	13.32(11)	0.92	14.67(07)	14.90(06)	--	
13	1	202	14.80(06)	0.83	59	17	15.94(18)	14.37(08)	0.74	15.39(04)	15.57(04)	1.67(03)	Etch 6
13	1	203	14.88(06)	0.82	56	19	15.70(15)	14.50(08)	0.75	15.42(04)	15.59(04)	2.08(05)	Etch 9
13	1	202	14.68(06)	0.83	61	15	15.78(22)	14.34(08)	0.78	15.32(04)	15.51(04)	1.83(11)	Etch 3
13	2	200	14.86(06)	0.79	58	16	15.53(18)	14.57(08)	0.76	15.41(04)	15.58(04)	1.50(06)	Etch 6
13	2	200	15.15(05)	0.73	56	17	15.65(16)	14.90(09)	0.71	15.61(04)	15.76(04)	1.70(04)	Etch 9
13	2	200	14.96(06)	0.80	33	141	15.60(22)	14.73(09)	0.78	15.51(04)	15.68(04)	1.19(07)	Etch 3
14	1	109	14.27(07)	0.75	60	16	14.87(26)	14.04(11)	0.73	14.99(05)	15.20(05)	--	TINT
14	1	41	14.22(14)	0.88	56	14	14.45(40)	14.12(19)	0.88	14.93(11)	15.15(10)	--	TINCLE
14	1	150	14.26(06)	0.79	59	15	14.75(22)	14.07(10)	0.78	14.97(05)	15.18(04)	1.45(03)	Combined
14	2	63	14.43(08)	0.60	58	13	15.01(39)	14.19(17)	0.58	15.10(06)	15.30(05)	--	TINT
14	2	38	14.81(10)	0.63	59	15	15.28(43)	14.62(20)	0.62	15.38(07)	15.56(07)	--	TINCLE
14	2	101	14.57(06)	0.64	58	14	15.10(29)	14.36(13)	0.62	15.20(05)	15.40(04)	1.60(03)	Combined
14	3	90	13.89(09)	0.89	57	16	14.71(27)	13.53(13)	0.85	14.68(07)	14.91(06)	--	TINT
14	3	70	14.18(14)	1.13	58	19	15.74(29)	13.56(13)	0.98	14.92(09)	15.13(08)	--	TINCLE
14	3	160	14.01(08)	1.01	57	17	15.20(20)	13.52(09)	0.92	14.78(05)	15.01(05)	1.27(04)	Combined
14	4	150	13.86(07)	0.84	60	16	14.60(23)	13.61(09)	0.82	14.70(05)	14.93(04)	1.28(04)	
16	1	100	14.42(09)	0.88	57	18	15.56(25)	13.92(12)	0.79	15.08(06)	15.28(06)	--	

20	1	109	13.15(12)	1.30	61	11	13.26(36)	13.11(14)	1.30	14.20(09)	14.50(08)	--	
21	A	255	13.85(06)	1.03	56	18	14.13(13)	13.71(08)	1.02	14.62(05)	14.84(05)	--	
21	B	212	13.71(07)	0.95	52	20	14.49(13)	13.23(08)	0.88	14.47(05)	14.69(04)	--	
21	C	125	12.71(18)	1.97	48	24	11.98(12)	13.37(12)	1.92	13.60(15)	13.85(14)	--	
21	D	273	14.72(05)	0.86	54	21	15.39(11)	14.35(07)	0.81	15.28(04)	15.45(04)	--	
21	E	268	13.18(06)	0.91	58	16	13.68(16)	12.98(07)	0.90	14.16(04)	14.44(04)	--	
22	1	120	13.45(06)	0.60	58	15	13.65(24)	13.36(12)	0.60	14.35(04)	14.61(04)	--	
23	1	100	14.02(07)	0.68	60	13	15.48(39)	13.54(13)	0.59	14.82(04)	15.05(04)	1.61(01)	
23	2	99	14.21(10)	0.97	60	18	14.58(24)	14.07(11)	0.96	14.94(08)	15.16(07)	--	
23	3	100	14.14(08)	0.81	57	18	14.56(22)	13.95(11)	0.79	14.86(06)	15.07(06)	1.93(01)	
24	1	104	14.18(06)	0.64	75	30	14.75(25)	13.99(10)	0.62	14.94(04)	15.16(04)	--	
25	1	100	10.08(22)	2.19	55	18	9.72(19)	10.30(13)	2.19	12.06(14)	12.53(14)	--	
26	1	100	13.92(08)	0.79	53	18	14.63(20)	13.51(12)	0.74	14.65(06)	14.87(05)	--	
28	1	100	13.94(09)	0.91	56	19	14.57(21)	13.63(12)	0.88	14.70(07)	14.92(06)	2.04(02)	
28	2	100	13.68(14)	1.37	55	21	14.78(20)	13.14(11)	1.29	14.51(09)	14.75(08)	2.04(02)	
30	1	105	13.93(09)	0.93	66	15	14.40(33)	13.81(10)	0.93	14.79(06)	15.04(06)	--	
30	2	100	12.86(11)	1.11	61	16	13.30(27)	12.71(12)	1.10	13.96(08)	14.26(08)	--	
32	1	100	13.87(08)	0.83	59	17	14.75(25)	13.55(11)	0.77	14.69(06)	14.93(05)	2.26(03)	aliquot a
32	1	101	13.86(09)	0.86	59	15	14.59(27)	13.58(12)	0.83	14.68(06)	14.91(06)	--	aliquot b
32	1	101	13.69(10)	1.01	58	17	14.23(24)	13.46(12)	0.99	14.53(08)	14.78(07)	--	aliquot c
32	2	101	14.26(08)	0.78	54	19	15.07(20)	13.82(12)	0.71	14.92(05)	15.12(05)	2.15(05)	aliquot a
32	2	101	14.51(09)	0.88	53	19	14.87(19)	14.30(12)	0.86	15.10(07)	15.28(06)	2.24(04)	aliquot b
32	2	101	14.33(07)	0.72	55	19	15.29(21)	13.87(11)	0.61	15.00(05)	15.20(04)	2.19(05)	aliquot c
32	3	110	14.68(08)	0.88	56	18	15.47(21)	14.31(11)	0.83	15.27(06)	15.45(06)	--	
32	4	100	14.23(11)	1.13	63	20	14.15(22)	14.26(11)	1.13	14.95(09)	15.16(08)	--	
34	1	100	14.37(09)	0.92	59	18	15.32(24)	14.01(11)	0.86	15.06(07)	15.26(06)	2.70(03)	
35	1	111	13.33(14)	1.49	60	15	14.30(30)	13.00(11)	1.46	14.34(09)	14.61(08)	1.78(04)	
37	1	50	14.26(07)	0.51	52	24	14.08(22)	14.37(17)	0.50	14.85(08)	15.03(08)	--	
38	1	100	14.16(12)	1.21	50	20	14.59(17)	13.87(13)	1.19	14.80(09)	14.99(09)	--	

39	1	80	14.98(08)	0.71	--	--	--	--	--	--	--	--	
41	1	100	14.54(08)	0.76	--	--	--	--	--	--	--	--	
41	2	100	14.43(08)	0.82	--	--	--	--	--	--	--	1.87(02)	
41	2	100	14.42(08)	0.80	--	--	--	--	--	--	--	--	Cf
41	3	100	14.01(09)	0.87	63	15	15.42(35)	13.63(11)	0.80	14.84(06)	15.07(05)	1.51(02)	
41	4	100	14.73(07)	0.69	62	12	15.67(41)	14.47(13)	0.67	15.36(05)	15.55(04)	1.92(02)	
41	5	100	14.31(09)	0.86	60	15	15.26(30)	13.99(11)	0.82	15.03(06)	15.24(06)	--	Cf
41	6	101	14.34(08)	0.77	63	11	15.25(44)	14.10(13)	0.76	15.08(05)	15.30(05)	--	
43	1	100	14.28(10)	1.04	--	--	--	--	--	--	--	--	
43	2	100	14.16(13)	1.27	--	--	--	--	--	--	--	--	
45	1	100	14.85(08)	0.79	--	--	--	--	--	--	--	2.32(02)	
47	1	100	13.72(09)	0.94	59	20	14.34(21)	13.45(11)	0.90	14.55(07)	14.79(07)	--	
47	2	100	13.64(09)	0.95	59	20	14.23(21)	13.39(11)	0.92	14.49(07)	14.73(07)	--	
47	3	106	13.73(12)	1.03	61	17	14.37(25)	13.51(11)	1.01	14.60(07)	14.85(07)	--	
